

We would like to thank the reviewers for their insightful commentary and catching the inconsistencies that existed in the first version. As a result, we have revised the manuscript substantially and believe it has significantly improved from its original submission. Please see the tracked changes revision attached to this review. One change that we made on our own volition was to develop a separate sub-category of the southeasterly cases that were either completely or predominantly southeasterly, and were either SDE days (i.e., 24 Feb and 10 Mar) or days with the most boundary layer influence based on the radon data (i.e., 27 Feb and 28 Feb). These days are indicated in green in the table, and figures and discussion has been revised to reflect this change.

Summary:

The results presented by M. Creamean and co-authors give insights into potential sources of INPs at the High Altitude Research Station Jungfraujoch. The study was conducted in winter and investigates freezing spectra of aerosol particles as derived from aerosol, cloud rime, and snow samples. The results from this study give an interesting insight into INP characteristics during this specific time at Jungfraujoch, however, my concerns center mostly around the methods used, which impact the interpretation of the results. After addressing these concerns and better highlighting the limitations of the study, the manuscript will be suitable for publication in ACP.

Major remarks:

- The results presented by Creamean et al. are based on a limited set of data with respect to sampling time. E.g. none of the southeasterly samples are within the free troposphere. This results in a confusion of air mass characteristics by wind direction versus in-or-out of boundary layer conditions. As such I believe the air masses cannot be distinguished as function of wind direction, which is one of the main findings of the authors. I suggest to better indicate which air mass is transported in the free troposphere and which is impacted by the boundary layer.

Actually, the southeasterly sample from 24 Feb was in the free troposphere as demonstrated by the radon data in the new Figure 1. To avoid confusion and as the reviewer suggests, we now clarify which cases (with the newly added boundary layer days of 27 Feb and 28 Feb) were affected by boundary layer air and which by the free troposphere. Table 1 now includes classifications for days under predominantly free tropospheric or boundary layer influences.

- Jungfraujoch is regularly exposed to short-term emissions from touristic activities, as e.g. tobacco smoke, emissions from helicopters and snow cats, as summarized in Bukowiecki et al., 2016. Such local emissions can lead to short-term peak concentrations of aerosol particles. Did you consider such emissions, especially with regard to the 24-hr aerosol sample? If not, this limits the interpretation of the results and should be pointed out.

Although it is possible such sources could affect the particle population, it is unlikely the 3 – 12 μm particles were affected by such local sources of pollution, given the typical size distributions of fresh cigarette smoke and combustion aerosol (e.g., Frohlich et al. (2015); Li and Hopke (1993); Zhang et al. (2013)). Bukowiecki et al. (2016) discuss these local source possibilities in the context of carbonaceous aerosol in PM_{10} . Although this is the case, we did add a statement to section 2.1: “It is possible local sources of aerosol, such as tobacco smoke or emissions from touristic infrastructure were collected by the DRUM (Bukowiecki et al., 2016), but did not likely affect the 2.96 – >12 μm particles which we focus on herein.

Fröhlich, R., Cubison, M. J., Slowik, J. G., Bukowiecki, N., Canonaco, F., Croteau, P. L., Gysel, M., Henne, S., Herrmann, E., Jayne, J. T., Steinbacher, M., Worsnop, D. R., Baltensperger, U., and Prévôt, A. S. H.: Fourteen months of on-line measurements of the non-refractory submicron aerosol at the

- Jungfraujoch (3580 m a.s.l.) – chemical composition, origins and organic aerosol sources. Atmos. Chem. Phys., 15, 11373-11398, doi:10.5194/acp-15-11373-2015, 2015.*
- Li, W., and Hopke, P. K.: Initial Size Distributions and Hygroscopicity of Indoor Combustion Aerosol-Particles, Abstr Pap Am Chem S, 206, 53-Envr, 1993.*
- Zhang, Y. P., Sumner, W., and Chen, D. R.: In Vitro Particle Size Distributions in Electronic and Conventional Cigarette Aerosols Suggest Comparable Deposition Patterns, Nicotine Tob Res, 15, 501-508, 10.1093/ntr/nts165, 2013.*

- Tracing air mass origin with the HYSPLIT model has some limitations in a complex terrain as Jungfraujoch. Another powerful tool to determine source emission sensitivities is FLEXPART, which is specifically improved for the site (e.g. Pandey Deolal et al., 2014). Given the spatial resolution of HYSPLIT I find it hard to thrust interpretations based on such results alone.

We use HYSPLIT in the context of the local meteorology and to support the aerosol and INP measurements. While we realize HYSPLIT has limitations in complex terrain, it has been widely used in a number of applications and can serve as a reliable (although, qualitative) tool to evaluate air mass sources. We wanted to use a simple tool to assess general air mass sources to corroborate local wind directionality and possible INP sources. One reason we ran trajectories at multiple ending altitudes was to assess any divergence in the results of general air mass transport direction. We also generalize all possible source locations within range of the trajectory pathways and are careful not to point at any one source. We have revised the second half of section 3.1 to insure we do not over interpret the results from HYSPLIT alone and solely use them to corroborate other in situ measurements.

- To my understanding the collection of cloud rime should only result in impaction of liquid water droplets on the collection plate, which freeze upon collision. In case that the cloud temperature is colder than the activation temperature of INPs, such samples should not contain ice-active particles. However, INP concentrations are very high in rime samples, and orders of magnitudes higher than the aerosol sample INP concentration. Please explain why this is the case.

For most of the time cloud temperature at the elevation of Jungfraujoch was warmer than -15 °C. Hence, the differences between rime and snow are small at temperatures below that. However, at cloud temperatures above -15 °C we generally found larger concentrations of INP in snow as compared to rime (Figure 7 in the initial manuscript, Figures 5 and 6 in revision). This finding supports your suggestion made in the second sentence of above paragraph. INP concentrations in rime differ from those in aerosol samples by orders of magnitude because INP concentrations in rime are per unit volume of liquid (rime melted for analysis) and those for aerosol are per unit volume of sampled air. Assuming a liquid water content of 0.1 g m⁻³ the INP concentrations in 1 L of rime are already seven orders of magnitude larger than those of aerosol in 1 L of air.

Specific remarks:

Page 1, title: Please specify that you investigate freezing spectra characteristics; readers outside of the INP community might get confused.

Done.

Page 1, lines 26 – 28 (and page 8, lines 284 – 285): I believe that with the methods used here, you cannot clearly identify biological, dust, or a mixture between the two. To make such connection in field studies would require a proper assessment of the aerosol particle population and/or of the ice residuals with respect to the biological and dust particle concentration.

This is based on the body of previous work, which we elaborate upon in the introduction. Hence, why we stated these are “punitive” influences and “possible” sources.

Page 1, line 30: This statement needs a reference.

These are widely accepted and understood processes that are quite broad in scope. We provide specific details under the umbrella of this statement in the following sentences, thus, did not think a citation was necessary for conventional wisdom.

Page 1, lines 33 – 34: The statement on the microphysical impact on precipitation formation in mixed-phase clouds needs a reference.

Done.

Page 3, lines 86 – 87: Before you defined “warm temperature INPs” as INPs active > -15°C (page 2, line 72). Please be consistent.

Fixed. Stopelli et al. (2016) used a different definition of warm temperature INPs, so we omitted their definition to avoid confusion.

Page 3, lines 97 – 98: Given the different temporal and spatial resolutions of your aerosol, cloud rime and snow samples, how can you explain the exchange of INPs into air, cloud, and precipitation? E.g. a 24-hr aerosol sample might not be dominated by the INP population which caused cloud and precipitation formation. Also, clouds might form far away from the site, as well as precipitation particles before reaching the ground.

The difference in temporal coverage between snow, rime, and aerosol sampling was due to practical constraints. It forces us to integrate in our interpretation over an air mass including clouds and cloud-free sections. As long as wind direction and planetary boundary layer influence are similar within an air mass, we think this approach can still lead to insights, although a perfect synchrony in sampling all components would of course have been preferable. We now address this issue at the end of section 2.1 (Aerosol, cloud rime and snow collection at Jungfraujoch).

Page 3, line 111: Please indicate if you refer to volume or mass/standard flow.

Fixed. Indicated this is volumetric flow.

Page 4, line 116: What is the collection efficiency of the drums? Is there a size dependency, e.g. an increased loss due to reflection on the stages for larger particles?

While we have not conducted our own tests for collection efficiency, the DRUM has been intercompared and characterized by previous work (e.g., Cahill et al. (1987); although they used an 8-stage DRUM). Although the study by Bukowiecki et al. (2009) presents testing of collection efficiency tests with a different DRUM model as ours (i.e., they used a 3-stage DRUM), they demonstrate how rotating drum impactors are generally accurate and robust. We have added these references to section 2.1.

Bukowiecki, N., Richard, A., Furger, M., Weingartner, E., Aguirre, M., Huthwelker, T., Lienemann, P., Gehrig, R., and Baltensperger, U.: Deposition Uniformity and Particle Size Distribution of Ambient Aerosol Collected with a Rotating Drum Impactor, Aerosol Sci Tech, 43, 891-901, 10.1080/02786820903002431, 2009.

Cahill, T. A., Feeney, P. J., and Eldred, R. A.: Size Time Composition Profile of Aerosols Using the Drum Sampler, Nucl Instrum Meth B, 22, 344-348, Doi 10.1016/0168-583x(87)90355-7, 1987.

Page 5, line 164: You introduce ^{222}Rn as abbreviation for radon, but you do not use it consistently in the text. Or do I miss a major difference between “radon” and “ ^{222}Rn ”?

We found one instance beyond the first time we introduce as “Radon (^{222}Rn)” in the text and the other time in the new Figure 1 caption where we just used “ ^{222}Rn ”. We have changed this to “radon” for consistency.

Page 5, line 177: You do not use the abbreviated “TSP” thereafter, therefore I suggest to not introduce it.

We have removed “TSP”.

Page 5, line 177: I do not understand why an increase in the 48-hour total suspended particle concentration is of interest in this study; given the time resolution of your rime and snow sample is on the order of hours, an overlap between a detected SDE (> 4 hours) and your sample might have occurred.

This information was based on previous work and the development of the Collaud-Coen et al. (2004) method for detecting SDEs at Jungfraujoch based on the PSI 48-h time resolution PM sampling. The purpose for providing this information is to demonstrate that SDEs do not always lead to substantially high concentrations of PM based on previous work. If 48-h PM value is not increased, then the SDE event was only a weak one or the temporal overlap with the 48-h period was short. We noted days where SDEs were detected, but that does not always translate to a day-long SDE. We have now clarified that this statement was based on previous work.

Page 5, lines 168 – 169: In previous studies several approaches have been used to assess boundary layer contact of the air mass arriving at Jungfraujoch. To make the distinction between boundary layer influence and free tropospheric conditions more reliable I suggest to use an additional method, as e.g. described by Herrmann et al., 2015.

We do not think the use of another boundary layer versus free tropospheric conditions method is necessary, as the radon provides in situ observational evidence of when the air arriving at Jungfraujoch was in contact with the boundary layer or not. Additionally, Herrmann et al. (2015) do use ^{222}Rn at Jungfraujoch and determine that it is “very much in line with the other two approaches” they used during their in-depth analysis. Thus, ^{222}Rn serves as a viable parameter for determining boundary layer influences at Jungfraujoch.

Page 6, lines 200 – 201: This is very vague, and not well quantified. A statistical analysis of e.g. mean travel height of the back trajectories for both wind directions would be helpful.

This contrasts with the reviewer’s previous comment on the limitations of HYSPLIT in complex terrain. This is the reason we generalize sources when considering the HYSPLIT results and only use them to provide some corroboration of local meteorology and the aerosol and INP results. We also compare the trajectories qualitatively and relative to each other. A more quantitative assessment would be speculative.

Page 6, line 220: What is the correlation coefficient? Is the relationship statistically significant?

The OPS and radon measurements do not necessarily correlate well when evaluating the highest time resolution of data available. What we intended to demonstrate with this statement was that when looking at a day at a time, we see relationships with increases and decreases during this time compared to before or after. We have revised this statement to reflect this intension.

Page 7, line 221: How do you determine upslope winds out of figure 1b?

We removed the word “upslope”.

Page 7, lines 236 – 237: Please add another reference for this quite general statement.

We have added Jaenicke (1980).

Jaenicke, R.: Atmospheric aerosols and global climate, Journal of Aerosol Science, 11, 577-588, [https://doi.org/10.1016/0021-8502\(80\)90131-7](https://doi.org/10.1016/0021-8502(80)90131-7), 1980.

Page 7, line 252 – 257: Figures 6c-h are hard to understand in the way they are visualized. Given that you do not observe any relationship between INP concentration and air temperature/wind speed, I suggest to show these results in the supplementary material.

We agree. We removed those from the figure (now the remaining panels are shown in the new Figure 6) and simply state that there was not relationship with wind direction and temperature.

Page 9, line 300: I cannot identify the freezing spectra for this case study. Please highlight this in e.g. figure 7.

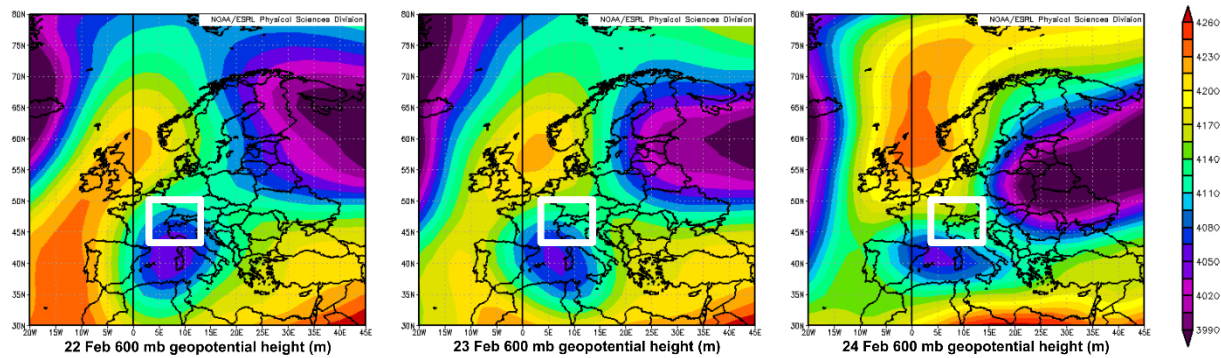
There is not one case that was discussed on page 9, line 300 (it was a continuation of discussing the air mass trajectories for 15 and 16 Feb). Spectral statistics including onset, T_{10} , T_{50} , and the warm and cold modal temperatures are presented in the new Figure 6, so one can glean how these days were different than the southeasterly or SDE and boundary layer case days.

Page 9, lines 300 – 302: I find it hard to follow your argumentation since you do not know the source region and transport pathway of the cloud.

We assume the air mass transport is not only characteristic of the air mass containing the INPs, but also the air mass containing clouds which likely formed during transport to Jungfrauoch. We have noted here, “...assuming the clouds formed along the air mass transport pathways.”

Page 9, lines 331 – 333: In order to strengthen this finding, you could include meteorological maps indicating frontal systems.

Unfortunately, we are not aware of any achieved meteorological maps containing such information (e.g., in situ radar) that are available free to the public. However, we looked at NCEP/NCAR reanalyses of 600 mb (approximate height of station) geopotential height (<https://www.esrl.noaa.gov/psd/data/composites/day/>), which corroborate the passing of a cold front from 22 Feb to 24 Feb to the southwest:



We have now indicated in the manuscript that the passage of a cold front was corroborated with NCEP/NCAR reanalysis. We also note in the methods that air mass transport was supported by NCEP/NCAR reanalyses of wind vectors and geopotential height at 600 mb (section 2.3).

Page 10, lines 354 – 368: This main part of your conclusion is rather open discussion, perspective and recommendation. I do not see relevant conclusions based on the presented results in this section.

This was intended to serve as broader context, which we did not originally clearly define by the section header. We have changed the name of this section to “Conclusions and broader implications” for clarity.

Page 18, figure 1: Apparently, the rime and snow collection time was often longer than the actual occurrence of the cloud event, since the grey shading in figure 1a indicated that the cloud events were lasting shorter than the sampling period (figure 1b). If so, please specify in the text.

We have revised this figure to show daily averages of cloud fraction but have indicated in the methods section (2.1) that sample collection sometimes lasted longer than cloud events.

Page 18, figure 1: The labels of the y-axis should not only contain the units, but also the property (e.g. “relative humidity (%)”)

Now that the revised Figure 1 has % of RH and cloud cover on the same axis, we did not specify, but rather added this information to the caption.

Using freezing spectra characteristics to identify ice nucleating particle populations during the winter ~~storms~~ in the Alps

Jessie M. Creamean^{1,2*}, Claudia Mignani³, Nicolas Bukowiecki^{4**}, Franz Conen³

¹Cooperative Institute for Research in Environmental Sciences, University of Colorado, Boulder, CO, USA

²Physical Sciences Division, National Oceanic and Atmospheric Administration, Boulder, CO, USA

³Department of Environmental Sciences, University of Basel, Switzerland

⁴Laboratory of Atmospheric Chemistry, Paul Scherrer Institute, Villigen, Switzerland

*Now at: Department of Atmospheric Science, Colorado State University, Fort Collins, CO, USA

**Now at: 3

Email: jessie.creamean@colostate.edu

Abstract. One of the least understood cloud processes is modulation of their microphysics by aerosols, specifically of cloud ice by ice nucleating particles (INPs). To investigate INP impacts on cloud ice and subsequent precipitation formation, measurements in cloud environments are necessary but difficult given the logistical challenges associated with airborne measurements and separating interstitial aerosol from cloud residues. Additionally, determining the sources of INPs is important given the dependency of glaciation temperatures on the mineral or biological components and diversity of such INP populations. Here, we present results from a comparison of INP spectral characteristics in air, cloud rime, and fresh fallen snow ~~for storm days~~ at the High-Altitude Research Station, Jungfraujoch. The goal of the study was two-fold: (1) to assess variability in wintertime INP populations found in-cloud based on air mass wind and air mass direction during snowfall and (2) to evaluate possible INP sources ~~s~~ between different sample types using a combination of cumulative INP ($K(T)$), normalized differential fraction frozen (df/dT), and normalized differential differential-INP spectra($k(T)$) spectra. INP freezing temperatures and concentrations were consistently higher on average from the southeast as compared to the northwest for rime, snow and especially aerosol samples which is likely a result of air mass influence from predominantly boundary layer terrestrial and marine sources in Southern Europe, the Mediterranean, and North Africa. For all three sample types combined, average onset freezing temperatures were ~~-8.07.7~~ and ~~-11.32~~ °C for southeasterly and northwesterly days, respectively, while $K(T)$ INP concentrations were 3 to 20 times higher when winds arrived from the southeast. Southeasterly aerosol samples typically had bimodal freezing spectra ~~a clear mode in the warm temperature regime~~ (i.e., ≥ -15 °C) in the df/dT and $k(T)$ spectra—indicating a putative influence from biological sources—while bimodality ~~the presence of a warm mode in~~ of the rime and snow varied ~~depending on meteorological context~~. Evaluating df/dT normalized concert with differential INP spectra- $k(T)$ spectra exhibited variable modality and shape—depending on the types of INPs present—and may serve as a viable-useful method for comparing different sampled ~~ing~~ substances and assessing the possible relative contributions of mixed mineral and biological versus only biological ~~contributions to INP~~ INP sample populations.

1 Introduction

Aerosols are key players in the atmospheric radiation budget, cloud microphysics, and precipitation development. ~~However, one of the most significant challenges with regard to aerosols is quantifying their impacts on cloud ice formation through serving as ice nucleating particles (INPs) (Boucher et al., 2013).~~ Aerosol-induced ice microphysical modifications influence cloud lifetime and albedo (Albrecht, 1989; Twomey, 1977; Storelvmo et al., 2011), as well as the production of precipitation (DeMott et al., 2010) ~~in clouds containing both liquid and ice~~. Mixed-phase clouds (MPCs) are ubiquitous in the troposphere over the entire annual cycle yet are difficult to quantify globally in part due to an inadequate understanding of aerosol-cloud interactions in mixed-phase

environments (Korolev et al., 2017). Thus, a close evaluation of aerosol-cloud processes is crucial to evaluating weather and climate processes. ~~;~~ However, one of the most significant challenges with regard to aerosols is quantifying their impacts on cloud ice formation through serving as ice nucleating particles (INPs) (Boucher et al., 2013). ~~however, e~~ Constraining aerosol-cloud impacts in models, specifically when parameterizing INPs in MPC systems, remains a significant challenge due to limited observations (Cziczo et al., 2017; Coluzza et al., 2017; DeMott et al., 2010; Kanji et al., 2017; Korolev et al., 2017). Observations ~~directly in cloudy environments~~ directly in-cloud are even more scarce—given the logistical costs and resources required by airborne platforms, caveats associated with aircraft probes and instrumentation, and instrumental artefacts caused by flying through clouds at high speeds (Cziczo et al., 2017)—but are ~~necessary-useful to assess for assessing~~ —the impacts of INPs on MPC microphysics as compared to most surface measurements which are geared towards evaluation of INP sources.

In the absence of conditions with -38°C and relative humidity with respect to ice above 140%, INPs are required for initiation of tropospheric cloud ice formation (Kanji et al., 2017). Aerosols such as dust and primary biological aerosol particles (PBAPs) are some of the most abundant and efficient INPs found in the atmosphere, respectively (Murray et al., 2012; Hoose and Möhler, 2012; DeMott et al., 1999; Conen et al., 2011; Creamean et al., 2013). PBAPs originating from certain bacteria, pollens, and vegetative detritus are the most efficient INPs known, capable of initiating freezing near -1°C , while most PBAPs (e.g., fungal spores, algae, and diatoms) tend to nucleate ice at temperatures similar to those of mineral dust (Despres et al., 2012; Murray et al., 2012; Tobo et al., 2014; Hader et al., 2014a; O'Sullivan et al., 2014; Hill et al., 2016; Tesson et al., 2016; Alpert et al., 2011; Knopf et al., 2010; Fröhlich-Nowoisky et al., 2015). In general, previous works collectively indicate that PBAP INPs that nucleate ice at temperatures greater than approximately -10°C are bacterial (Murray et al., 2012; Hu et al., 2018; Hoose and Möhler, 2012; Despres et al., 2012; Fröhlich-Nowoisky et al., 2016), but could also be pollen or certain fungal spores (von Blohn et al., 2005; Hoose and Möhler, 2012; O'Sullivan et al., 2016), although the latter two are less likely. Plant bacteria such as *Pseudomonas syringae* are deemed omnipresent in the atmosphere and precipitation (Despres et al., 2012; Stopelli et al., 2017; Morris et al., 2014), and facilitate cloud ice formation up to -1°C (Despres et al., 2012). While, only a few laboratory-based studies have reported known inorganic or mineral materials ~~that with~~ ice nucleation activity at such temperatures (Ganguly et al., 2018; Atkinson et al., 2013). Mineral and soil dust serving as atmospheric shuttles for organic microbial fragments can be transported thousands of kilometres and serve as effective INPs, even from highly arid regions such as the Sahara (Kellogg and Griffin, 2006). ~~The, yet the exact~~ origin of the ice nucleation germ forming at the warmest temperatures is speculated-thought to be due to the ice binding proteins or macromolecules of the biological components in mixed mineral-biological INPs (O'Sullivan et al., 2014; O'Sullivan et al., 2016; Conen and Yakutin, 2018). In general, the previous studies on the climate relevance of PBAPs demonstrate the importance of such INPs at MPC temperatures and precipitation enhancement (Morris et al., 2004; Bergeron, 1935; Christner et al., 2008; Morris et al., 2014; Morris et al., 2017; Stopelli et al., 2014; Fröhlich-Nowoisky et al., 2016).

Although biological constituents, from cellular material to in-tact bacteria and spores, are thought to be omnipresent in the atmosphere (Burrows et al., 2009b; Burrows et al., 2009a; Jaenicke, 2005; Jaenicke et al., 2007), modeling studies constraining global emission estimates of biological INPs and PBAPs are very limited, subject to significant hurdles, and often yield conflicting results due to ~~the dearth of~~ not having a sufficient set of observations and complexity of atmospheric PBAPs (Hummel et al., 2015; Burrows et al., 2013; Twohy et al., 2016; Fröhlich-Nowoisky et al., 2012; Despres et al., 2012; Hoose and Möhler, 2012; Morris et al., 2011). Yet, biological aerosols such as bacteria have been shown to cause significant perturbations in cloud ice in numerical weather prediction models, affording modulations in cloud radiative forcing and precipitation formation (Sahyoun et al., 2017). In addition, measuring and quantifying PBAPs is non-trivial—methodologies for counting, culturing, and nucleic acid sequencing of PBAPs and especially for those which fall in the warm temperature INP regime (i.e., INPs that nucleate ice $> -15^{\circ}\text{C}$) are: (1) time

79 and labor intensive, (2) require specific expertise or at times substantial resources, (3) require substantial sample volumes, or (4)
80 are species- or genera-specific or limited to viable microorganisms (Despres et al., 2012). Although such techniques are required
81 to adequately assess the atmospheric microbiome and PBAP sources, a simpler approach could be applied to evaluate and even
82 quantify warm temperature biological INP populations as compared to colder temperature PBAPs or mineral dust.

83 The ~~goal-objectives~~ of the study presented here ~~focuses on are~~: (1) to conduct an intercomparison of INP measurements of aerosol,
84 cloud rime, and snow directly ~~in-cloud and in-cloud environments at the ground~~ and (2) ~~evaluating-evaluate different types of~~ INP
85 spectra in a manner such that we can estimate the relative contribution from biological INPs in the warm temperature regime
86 relevant to MPCs. Sampling was conducted at the High-Altitude Research Station Jungfraujoch (JFJ), a unique location for
87 evaluating populations of INPs that affect winter storms in the European Alps, and where MPCs are particularly common
88 (Lohmann et al., 2016). Recent studies at JFJ have provided valuable insight into INP concentrations, sources, and removal
89 processes under a variety of conditions and during various times of the year. Conen et al. (2015) measured INPs at -8°C over the
90 course of a year at JFJ, and found a strong seasonality in such INPs, with two order of magnitude higher concentrations observed
91 during the summer. They also suggested INPs measured at this temperature may be limited most of the year by microphysical
92 processing during transit. Stopelli et al. (2015) verified this removal mechanistic process through INP measurements and isotopic
93 composition of fresh fallen snow at JFJ, concluding that warm temperature ~~INPs (i.e., INPs active at $> -10^{\circ}\text{C}$)~~ are rapidly depleted
94 by precipitating clouds at lower elevations. Stopelli et al. (2016) expanded their INP analyses to 2-years of data at JFJ, concluding
95 that a high abundance of INPs at -8°C is to be expected whenever high wind speed coincides with air masses having experienced
96 little or no precipitation prior to sampling, yet a separate study by Stopelli et al. (2017) found that only a small fraction of the INPs
97 were ~~bacterial-cultivable~~ cells of *Pseudomonas syringe*. In contrast, Lacher et al. (2018a; 2018b) conducted an interannual synopsis
98 of INP measurements at JFJ and found anthropogenic influence on INP concentrations, but only during boundary layer intrusion
99 (BLI) influences and at relatively cold temperatures (i.e., approximately -30°C), and higher INP concentrations during Saharan
100 dust events (SDEs) and marine boundary layer air arriving at JFJ. Eriksen Hammer et al. (2018) characterized ice particle residuals
101 and concluded that silica and aluminosilicates were the most important ice particle residuals at JFJ during the mixed-phase cloud
102 events during Jan – Feb 2017, while carbon-rich particles of possible biological origin were ~~of a~~ minor contribution.

103 Here, we demonstrate how variable sources influence INP populations depending on air mass transport and ~~storm~~ direction, and
104 spectral modality between the rime, snow, and aerosols can help explain the exchange of INPs from air into cloud then into
105 precipitation. Our results expand upon previous studies by evaluating INPs via a combination of aerosol, rime, and snow, and at a
106 temperature range that comprises common biological and mineral INPs.

107 2 Methods

108 2.1 Aerosol, cloud rime and snow collection at Jungfraujoch

109 Collocated collection of snow, cloud rime, and aerosol samples for the Ice Nucleation Characterization in the Alps of Switzerland
110 (INCAS) study took place 15 Feb – 11 Mar 2018 in the Sphinx observatory at JFJ (46.55°N , 7.98°E ; 3580 m above sea level (m
111 a.s.l.); <https://www.hfsjg.ch/en/home/>). Snow was collected as described by Stopelli et al. (2015) using a Teflon-coated tin (0.1
112 m^2 , 8 cm deep) for a duration of 1 – 18 hours, but typically for 1 – 4 hours. Collection quantities and inherent time of collection
113 were dependent upon snowfall rates but additionally on winds blowing snow out of the collection pans. Because of this possibility,
114 we cannot determine actual snowfall rates with certainty. Cloud rime was collected using a slotted plexiglass plate placed vertically
115 during snow sample collection (Lacher et al., 2017; Mignani et al., 2018). Sample collection times were at times longer than the

116 duration of in-cloud conditions (see section 2.3) and were dependent on when manually changing the sampling tin and plate was
 117 possible. Daily size-resolved aerosol samples were collected using a Davis Rotating-drum Universal-size-cut Monitoring (DRUM)
 118 single-jet impactor (DA400, DRUMAir, LLC.) (Cahill et al., 1987; Bukowiecki et al., 2009; Creamean et al., 2018a) ~~as described~~
 119 ~~by Creamean et al. (2018a)~~ from a 1-m long inlet constructed of 6.4-mm inner diameter static-dissipative polyurethane tubing
 120 (McMaster-Carr®) leading to outside of the Sphinx and connected to a funnel covered with a loose, perforated plastic bag to
 121 prevent rimed ice build-up or blowing snow from clogging the inlet. The DRUM collected aerosol particles at four size ranges
 122 (0.15 – 0.34, 0.34 – 1.20, 1.20 – 2.96, and 2.96 – >12 µm in diameter) and sampled at 27.7 L min⁻¹ (volumetric flow), equalling
 123 39888 total L of air per sample. Such size ranges cover a wide array of aerosols—particularly those that serve as INPs (DeMott et
 124 al., 2010; Fridlind et al., 2012; Mason et al., 2016)—while the large volume of air collected promotes collection of rarer, warm
 125 temperature biological INPs, but may represent a lower fraction of overall INP concentrations (Mossop and Thorndike, 1966).
 126 Samples were deposited onto 20 x 190 mm strips of petrolatum-coated (100%, Vaseline®) perfluoroalkoxy plastic (PFA, 0.05 mm
 127 thick) substrate secured onto the rotating drums (20 mm thick, 60 mm in diameter) in each of the four stages at the rate of 7 mm
 128 per day (5 mm of sample streaked onto the PFA followed by 2 mm of blank). It is possible local sources of aerosol, such as tobacco
 129 smoke or emissions from touristic infrastructure, were collected by the DRUM (Bukowiecki et al., 2016), but did not likely affect
 130 the 2.96 – >12 µm particles which we focus on herein. Intervals in which snow, rime, and aerosol were sampled did not fully
 131 overlap during a day because conditions were changing often unpredictably between out-of-cloud and in-cloud conditions, the
 132 latter with or without precipitation. At the same time we intended to collect enough material from either component for a robust
 133 analysis of warm temperature INPs. Consequently, the combined data of a day integrate over a larger air mass, including clouds
 134 and cloud-free regions. Comparing data from snow, rime, and aerosol samples still makes sense as long as wind direction and the
 135 influence of planetary boundary layer did not change substantially during a day.

136 2.2 Ice nucleation measurements

137 All samples were analysed immediately after collection for INPs using a drop freezing cold plate system described by Creamean
 138 et al. (2018b; 2018a). Briefly, snow and cloud rime samples were melted into covered 50-mL glass beakers for analysis, resulting
 139 in approximately 10 mL of liquid per sample. Samples were manually shaken prior to analysis. Aerosols deposited onto the PFA
 140 were prepared for drop freezing by cutting out each daily sample and placing in a 50-mL glass beaker with 2 mL of molecular
 141 biology reagent grade water (Sigma-Aldrich®). Beakers were covered and shaken at 500 rpm for 2 hours (Bowers et al., 2009). In
 142 between sampling, beakers were cleaned with isopropanol (99.5%), sonicated with double-distilled water for 30 minutes, ~~then and~~
 143 then heated at 150 °C for 30 minutes.

144 Copper discs (76 mm in diameter, 3.2 mm thick) were prepared by sonicating in double-distilled water for 30 minutes, cleaning
 145 with isopropanol, then coated with a thin layer of petrolatum (Tobo, 2016; Bowers et al., 2009). Following sample preparation, a
 146 sterile, single-use syringe was used to draw 0.25 mL of the suspension and 100 drops were pipetted onto the petrolatum-coated
 147 copper disc, creating an array of ~2.5-µL aliquots. Drops were visually inspected for size; however, it is possible not all drops were
 148 the same exact volume, which could lead to a small level of ~~indeterminable undetermined~~ uncertainty. ~~However, previous studies~~
 149 ~~have demonstrated that drop size variability within this range does not significantly impact freezing results~~ (Hader et al., 2014b;
 150 Bigg, 1953; Langham and Mason, 1958; Creamean et al., 2018b). The copper disc was then placed on a thermoelectric cold plate
 151 (Aldrich®) and covered with a transparent plastic dome. Small holes in the side of the dome and copper disc permitted placement
 152 of up to four temperature probes using an Omega™ thermometer/data logger (RDXL4SD; 0.1 °C resolution and accuracy of ±
 153 (0.4% + 1 °C) for the K sensor types used). During the test, the cold plate was cooled at 1 – 10 °C min⁻¹ from room temperature
 154 until around –35 °C. Control experiments at various cooling rates within this range show very little discernible dependency of

155 drop freezing on cooling rate (Creamean et al., 2018b), akin to previous works (Wright and Petters, 2013; Vali and Stansbury,
156 1966).

157 A +0.33 °C correction factor was added to any temperature herein and an uncertainty of 0.15 °C was added to the probe accuracy
158 uncertainty based on DFCP characterization testing presented in Creamean et al. (2018b), to account for the temperature difference
159 between the measurement (i.e., in the plate centre) and actual drop temperature. Frozen drops were detected ~~visually, but~~ visually
160 ~~but~~ recorded through custom software. The software records the time, probe temperature, and cooling rate for every second of the
161 test. When a drop is identified as frozen, a button is clicked on the software graphical user interface so that it records that exact
162 time, probe temperature, and cooling rate of that drop in a separate file, providing the freezing temperature and cooling rate of each
163 drop frozen. The test continued until all 100 drops were frozen. Each sample was tested three times with 100 new drops for each
164 test. ~~From each test, the fraction frozen and percentage of detected frozen drops were~~ calculated from all detected drops
165 frozen combined from the three tests (typically, > 90% of the drops were detected). The results from the triplicate tests were then
166 binned every 0.5 °C to produce one spectrum per sample. ~~Normalized differential INP spectra were created by a using a~~
167 ~~combination of calculations. First, cumulative INP spectra concentrations~~ were calculated using the equation ~~posed by~~ from Vali
168 (1971):

169
$$[INPs(T)]K(TL^{-1}) = -\frac{1}{V_{drop}} \times \ln[1 - f(T)] \frac{\ln N_0 - \ln N_u(T)}{V_{drop}}$$

170 Where V_{drop} is the average volume of each drop and $f(T)$ is the fraction of drops frozen at temperature T . N_0 is the total number of
171 drops, $N_u(T)$ is the number of unfrozen drops at each temperature, and V_{drop} is the average volume of each drop. Normalized
172 differentials of the frequency of freezing events, or df/dT , were calculated finding the difference in $f(T)$ at each temperature bin of
173 0.5 °C and normalizing to the maximum df/dT value per sample, then smoothed using a moving average. Aerosol cumulative INP
174 concentrations were corrected for the total volume of air per sample (~~$INPsK(T) \times \frac{V_{suspension}}{V_{air}}$~~) while melted rime/snow residual
175 cumulative INPs were adjusted to the total used during analysis ($K(T)INPs \times V_{suspension}$), where $V_{suspension}$, $V_{suspension}$ and V_{air} , V_{air}
176 represent the total liquid volume analyzed per sample (0.75 mL for the three tests) and total volume of air drawn per sample (39888
177 L), respectively.

178 ~~Second, differential values were calculated from each 0.5 °C cumulative concentration. Differential INP spectra—which as the~~
179 ~~name indicates, correspond to the differential of the cumulative spectra (Vali et al., 2015)—were used early in earlier studies (Vali,~~
180 ~~1971; Vali and Stansbury, 1966), however, spectra from these previous studies only reached a minimum of -20 °C due to the~~
181 ~~limitations of background artifacts in the water used at that time, missing the tail end of what are usually the highest INP~~
182 ~~concentrations as discussed in more detail below. Recent work by Vali (2018) revisits the use of differential spectra, expanding to~~
183 lower temperatures. We employ the calculation for differential INP concentrations from Vali (2018):

184
$$k(T) = -\frac{1}{V_{drop} \times \Delta T} \times \ln\left(1 - \frac{\Delta N}{N(T)}\right)$$

185 where N is the number of unfrozen drops and ΔN is the number of freezing events observed between T and $(T - \Delta T)$. Third,
186 differential concentrations were divided by the maximum concentration per sample (i.e., to normalize). Last, then spectra were
187 smoothed using a moving average.

2.3 Supporting meteorological and source analysis data

Auxiliary surface meteorological observations, including but not limited to hourly mean air temperature measured 2 m above ground level (a.g.l.) ($^{\circ}\text{C}$), relative humidity measured 2 m a.g.l. (%), scalar wind speed (m s^{-1}) and direction (degrees), and incoming longwave radiation (W m^{-2}) were acquired from MeteoSwiss (<https://gate.meteoswiss.ch/idaweb/>). From the longwave measurements, in-cloud conditions were determined by calculating the sky temperature and comparing to air temperature measured at the station, per the methodology of Herrmann et al. (2015) from a 6-year analysis of JFJ observations. There were no in situ measurements of cloud presence or extent. For the current work, each hourly measurement was categorized as out-of-cloud or in-cloud based on such ~~calculations~~ calculations and averaged to obtain daily cloud coverage percentage.

Radon (^{222}Rn) concentrations have been continuously measured at JFJ since 2009. Details on the detectors themselves and the measurements can be found in Griffiths et al. (2014). Briefly, 30-minute radon concentrations were measured using a dual-flow-loop two-filter radon detector as described by Chambers et al. (2016). Calibrated radon concentrations were converted from activity concentration at ambient conditions to a quantity which is conserved during an air parcel's ascent: activity concentration at standard temperature and pressure (0°C , 1013 hPa), written as Bq m^{-3} STP (Griffiths et al., 2014). Time periods with ~~boundary-layer~~ BLI intrusion were classified as radon concentrations $> 2 \text{ Bq m}^{-3}$ (Griffiths et al., 2014). Particle concentrations from approximately 0.3 to $> 20 \mu\text{m}$ in diameter were measured with a 15-channel optical particle sizer (OPS 3300; TSI, Inc.) at a 1-minute time resolution (Bukowiecki et al., 2016). Due to operational complications, ~~OPSC~~ data were not collected prior to 23 Feb during INCAS. Air was drawn through a heated total aerosol inlet (25°C) which, besides aerosol particles, enables hydrometeors with diameters $< 40 \mu\text{m}$ to enter and to evaporate, at wind speeds of 20 m s^{-1} (Weingartner et al., 1999). SDEs were determined from existing methodology using various aerosol optical properties, but specifically, the Ångström exponent of the single scattering albedo (α_{SSA}), which decreases with wavelength during SDEs (Collaud Coen et al., 2004; Bukowiecki et al., 2016). SDEs are automatically detected by the occurrence of negative α_{SSA} that last more than four hours. Based on previous work, mMost of the SDEs do not lead to a detectable increase of the 48-h total suspended particulate matter (~~TSP~~) concentrations at JFJ (Collaud Coen et al., 2004). Additionally, we consider these events probable SDEs, but may have influences from other sources in addition.

Air mass transport analyses were conducted using the HYbrid Single Particle Lagrangian Integrated Trajectory model with the SplitR package for RStudio (<https://github.com/rich-iannone/SplitR>) (Draxler, 1999; Draxler and Rolph, 2011; Stein et al., 2015). Reanalysis data from the National Centers for Environmental Prediction (NCEP) National Center for Atmospheric Research (NCAR) (2.5° latitude-longitude; 6-hourly; https://www.ready.noaa.gov/gbl_reanalysis.php) were used as the meteorological fields in HYSPLIT simulations. Air mass transport directionality and frontal passages were verified by NCEP/NCAR reanalyses of wind vectors and geopotential height at 600 mb (i.e., approximate pressure at the altitude of JFJ; <https://www.esrl.noaa.gov/psd/data/composites/day/>). Trajectories were initiated at 10, 500, and 1000 m a.g.l. every 3 hours daily, but only the 500-m trajectories are shown. Trajectories were only simulated for each northwesterly, ~~and~~ southeasterly, SDE, and BLI case study day (i.e., Table 1). It is important to note that “northwesterly” is a contribution of north, west, and northwest winds, while “southeasterly” includes south, east, and southeast winds. SDE and BLI days were predominantly (not entirely) southeasterly.

3 Results and discussion

3.1 Directional dichotomy of ~~storm systems~~ air masses arriving at JFJ during INCAS

Local surface meteorology was variable at JFJ during INCAS, with air temperatures ranging from -27.5 to -4.8 °C (average of -13.7 °C)—temperatures relevant to heterogeneous nucleation of cloud ice—and relative humidity ranging from 18 to 100% (Figure 1a). ~~All days contained some fraction of in-cloud conditions that varied between 12% and 100%, on average. Wind speed was 6.4 m s^{-1} on average, with spikes during most storm systems up to 22.8 m s^{-1} (i.e., wind speed during rime and snow collection; Figure 1b).~~ Due to the topography surrounding JFJ, predominant wind directions were northwest followed by southeast, with the fastest winds recorded originating from the southeast (Figure 2) (Figure 2). Such conditions are typical for JFJ during the winter (Stopelli et al., 2015; Collaud Coen et al., 2011). Out of the entire study, several days were classified as northwesterly (5 days) or southeasterly (2 days) ~~during storm~~ conditions when a combination of aerosol, cloud rime, and snow samples were collected (i.e., a full 24 hours of northwesterly or a full 24 hours of southeasterly winds during snowfall; Table 1), which are herein focused on as the case study days (indicated by the blue and red in Figure 1b, respectively). ~~These days were also deemed days with “storm” conditions since clouds and snow were both present at JFJ. There were 4 days that maintained predominantly southerly wind directions as indicated in green in Figure 1b and Table 1 and were characterized as days influenced by SDEs or BLI as discussed herein. Rime and snow were only collected on one of these days, while remaining SDE or BLI cases had only aerosol collected. Aside from 22 Feb (missing data), the remaining days in the study were characterized as FT and did not exhibit influences from warm temperature INPs (see section 3.2 and 3.3).~~

~~Most southeasterly case days (and 06 Mar) apart from the SDE days experienced longer residence times in what was likely the boundary layer (i.e., 1000 m or less) compared to northwesterly cases, which is supported by radon data (Figure 1c). Griffiths et al. (2014) determined that radon concentrations $> 2 \text{ Bq m}^{-3}$ signify BLI, which in the current work was clearly observed on 23 Feb, 27 Feb, 28 Feb, 06 Mar, and 11 Mar case days, indicating samples collected on these days were likely influenced by continental boundary layer sources. Relatively low radon concentrations were observed the remaining case study days, indicating these samples were predominantly affected by free tropospheric (FT) air and thus, lower aerosol concentrations and/or more distant, including marine, sources. Although OPS data were missing until 23 Feb, source information can be gleaned from the available data. For example, 23 Feb had episodic high concentrations of particles (maximum of 9.6 cm^{-3}) towards the beginning of the day coincident with the largest spike in radon, with a steady decrease as time transpired, indicating the boundary layer was an ample source of $> 0.3 \text{ }\mu\text{m}$ particles. A similar episode with the OPS and radon concentrations was observed 27 – 28 Feb, where the highest concentrations of each were observed during the entire study period. Selected days were subject to diurnal winds (not shown), such as 06 Mar, where boundary layer air reached JFJ and a midday maximum in OPS particle concentrations was observed, indicating lower elevations were the dominant source of aerosol. Although, diurnal variations in aerosol from local sources have been shown to not be common in the winter at JFJ (Baltensperger et al., 1997). In contrast, 11 Mar was exposed to boundary layer air based on radon observations, but particle concentrations were low (average of 0.2 cm^{-3} compared to a study average of 3.0 cm^{-3}), signifying that although BLI occurred at JFJ, it was not a substantial source of aerosol. These relationships corroborate the ice nucleation observations, as discussed in detail below.~~

Extending past local conditions, air mass transport 10 days back in time prior to reaching JFJ on case study days was, as expected, dissimilar between northwesterly (Figure 3) and southeasterly/SDE/BLI (Figure 4) conditions. The main distinctions between northwesterly and southeasterly/SDE/BLI days are: (1) northwesterly days originated from farther west, with some days reaching back to ~~the Canadian Archipelago~~ North America, while air masses on southeasterly/SDE/BLI days predominantly hovered over

land and ~~occasional~~ oceanic sources closer to Europe, (2) southeasterly SDE/BLI air masses travelled closer to the surface relative to northwesterly days, ~~especially south and east of JFJ~~ while northwesterly air masses were typically transported from higher altitudes (i.e., more ~~free tropospheric~~ FT exposure), and (3) aside from 06 Mar (which is discussed in more detail in the following section), northwesterly air masses did not travel over the Mediterranean and northern Africa, whereas the southeasterly SDE/BLI air masses ~~reaching down to 100 m~~ above JFJ arrived from over such regions within less than 2 days before arriving to JFJ. One obvious inconsistency is that the air mass trajectories on 24 Feb do not indicate transport occurred from Northern Africa even though this day was characterized as an SDE. Collaud Coen et al. (2004) reported that in 71% of all cases they evaluated at JFJ, 10-day back-trajectories were able to reveal the source of Saharan dust and that back trajectories cannot always explain SDEs. Boose et al. (2016) reported similar transport pathways for JFJ during multiple consecutive winters and concluded that marine and Saharan dust served as dominant sources of INPs at -33 °C. Reche et al. (2018) also reported similar pathways and sources for bacteria and viruses, but during the summer in southern Spain. ~~Possible SDEs were automatically detected on 24 Feb and 10 Mar in the current work, and air mass transport pathways are shown for these days.~~ These disparate sources and transport pathways of air support the variability in the ice nucleation observations as discussed in more detail in the following section.

~~As evidenced by the air mass transport analyses, each southeasterly case day (and 06 Mar) experienced longer residence times in what was likely the boundary layer (i.e., 1000 m or less) compared to northwesterly cases, which is supported by ²²²Rn data (Figure 5). Griffiths et al. (2014) determined that radon concentrations $> 2 \text{ Bq m}^{-3}$ signify boundary layer intrusion, which in the current work was clearly observed on 23 Feb, 06 Mar, and 11 Mar, indicating samples collected on these days were likely influenced by boundary layer sources (planetary and marine). Relatively low radon concentrations were observed the remaining case study days, indicating these samples were predominantly affected by free tropospheric air and thus, lower aerosol concentrations and/or more distant sources. Although OPC data were missing until 23 Feb, source information can be gleaned from the available data. For example, 23 Feb had episodic high concentrations of particles (maximum of 9.6 cm^{-3}) towards the beginning of the day coincident with the largest spike in radon, with a steady decrease as time transpired, indicating the boundary layer was an ample source of $> 0.3 \text{ }\mu\text{m}$ particles. Although not a case study time period, a similar correlation between the OPC and radon concentrations was observed 27–28 Feb, where the highest concentrations of each were observed during the entire study time period. Selected days were subject to diurnal upslope winds (Figure 1b), such as 6 Mar, where boundary layer air reached JFJ and a midday maximum in OPC particle concentrations was observed, indicating lower elevations were the dominant source of aerosol. Although, diurnal variations in aerosol from local sources have been shown to not be common in the winter at JFJ (Baltensperger et al., 1997). In contrast, 11 Mar was exposed to boundary layer air based on radon observations, but particle concentrations were low (average of 0.2 cm^{-3} compared to a study average of 3.0 cm^{-3}), signifying that although boundary layer intrusion occurred at JFJ, it was not a substantial source of aerosol. These relationships corroborate the ice nucleation observations, as discussed in detail below.~~

289 **3.2 Variability in INP spectra** ~~1-properties based on storm air mass characteristics~~ source

290 Out of the 25 aerosol, 30 rime, and 39 snow samples collected, 7 aerosol, 19 rime, and 23 snow were collected northwesterly or
 291 southeasterly storm case study days, while 4 aerosol, 1 rime, and 2 snow were collected on SDE or BLI days (Table 1). Most
 292 mMixed wind direction days were excluded, as sources from both directions would contribute to the daily aerosol sample. Figure
 293 56 shows the cumulative ($K(T)$) INP concentrations, normalized differential fraction frozen per $0.5 \text{ }^{\circ}\text{C}$ temperature interval (df/dT),
 294 and normalized differential ($k(T)$) INP concentrations from aerosol, snow, and rime samples on the case days ~~compared to air~~
 295 ~~temperature, wind speed, and previous measurements at JFJ. The use of df/dT while qualitative and possibly method-specific in~~
 296 terms of modality locations, demonstrates the presence of 1 – 2 INP populations by having a mode in the warm regime (i.e., warm

mode or likely primarily biological) and/or cold regime (i.e., $< 15^{\circ}\text{C}$; cold mode or likely a mixture of mineral and biological) (Augustin et al., 2013) and enables us to intercompare between the different types of samples.

In addition to containing higher concentrations of warm temperature INPs, most southeasterly and SDE/BLI samples contained a clear mode in the warm temperature regime compared to northwesterly samples which typically did not contain such a mode in the df/dT and $k(T)$ spectra. This warm mode, or “bump” at temperatures above approximately -15°C has been observed in a wide range of previous immersion mode ice nucleation studies including but not limited to some of the earliest studies of total aerosol (Vali, 1971), residuals found in hail (Vali and Stansbury, 1966), sea spray aerosol (McCluskey et al., 2017; DeMott et al., 2016), soil samples (Hill et al., 2016), agricultural harvesting emissions (Suski et al., 2018), and in recent reviews of aerosol (Kanji et al., 2017; DeMott et al., 2018) and precipitation (Petters and Wright, 2015) samples. Most previous studies that show spectra with the warm mode typically: (1) report a wide range of freezing temperatures such that it can be observed relative to the steady increase of INPs at colder temperatures or (2) are of samples that include a mixture of biological and mineral or other less efficient INP sources. For example, several previous studies report INP concentrations down to only -15°C (e.g., Conen and Yakutin, 2018; Hara et al., 2016; Kieft, 1988; Schnell and Vali, 1976; Vali et al., 1976; Wex et al., 2015), namely because the goal was to target efficient, warm-temperature biological INPs. However, the warm mode may not be evident in such studies, given it cannot be visualised next to the drastic increase in INPs with temperatures below -15°C (i.e., the cold mode). In contrast, studies conducting INP measurements on known mineral dust samples also are not able to observe the warm mode (e.g., Price et al., 2018; Atkinson et al., 2013; Murray et al., 2012). Together, it is apparent that a mixed biological and mineral (or less efficient biological INPs) sample is needed to assess the modal behaviour in the INP spectra.

Only the largest size range of the aerosol is shown because the remaining size ranges (i.e., $< 2.96\text{ }\mu\text{m}$) were not distinct with respect to wind direction. The fact that size, alone, exhibited directionally-dependent results and that such dependencies were only observed in the coarse mode aerosol indicate: (1) the sources were indeed different between northwesterly, ~~and~~ southeasterly, and SDE/BLI transport—supporting the air mass source analyses—and (2) the coarse mode aerosols were likely from a regional source as opposed to long-range transported thousands of kilometres. This is because gravitational settling typically renders transport of coarse particles inefficient especially within the boundary layer (Creamean et al., 2018a; Jaenicke, 1980). Previous work by Collaud Coen et al. (2018) concludes that the local boundary layer ~~never infrequently~~ influences JFJ in the winter, supporting ~~the fact that regional sources were likely prominent in the current work~~ the current work (i.e., more FT days (17 of 25 days); Table 1).

Generally, INPs from southeasterly and SDE/BLI days were higher in concentration and more efficient (i.e., were warm temperature INPs that facilitated ice formation $> -15^{\circ}\text{C}$) than northwesterly samples. Our results are parallel to those by Stopelli et al. (2016), who also observed higher $K(T)$ INP concentrations in snow samples collected during southerly conditions at JFJ from Dec 2012 to Oct 2014 (Figure 6a). However, $K(T)$ when comparing overlapping temperature ranges from the snow samples during the winter only (Figure 6a), concentrations reported here ~~are were~~ generally higher than those reported by Stopelli et al. (2016), especially for the northwesterly samples at the highest temperatures. Unlike Stopelli et al. (2016), there was no clear correlation between $K(T)$ with air temperature and wind speed in the current work (not shown).

~~Aside from some of the snow samples, o~~ Onset freezing temperatures (i.e., the highest temperature in which the first drop in each sample froze) were typically higher for ~~samples from the~~ southeasterly/SDE/BLI samples—as compared to the northwest (Figure 6b), indicating influences from ~~more efficient INP sources that produce warm temperature INPs on these days, from the southeast.~~ The temperatures in which 10% (T_{10}) and 50% (T_{50}) of the samples froze were also typically higher for the southeast/SDE/BLI as

334 compared to the northwest samples, especially for the aerosol samples, indicating higher concentrations of more efficient warm
335 temperature INPs. However, a larger (smaller) spread in onset temperatures was observed in samples from the northwest
336 (southeast), suggesting two possibilities: (1) influences were more (less) variable sources from the northwest (southeast), as
337 discussed in more detail in the following section and/or (2) in the case of cloud rime and snow, clouds from the northwest were
338 already depleted with the most efficient INPs due to precipitation prior to arriving at JFJ (i.e., higher transport altitudes which
339 could have been exposed to cloudy conditions as compared to the southeast days which exhibited transport closer to the ground;
340 Figures 3 and 4).

341 There was no clear correlation between *INP concentrations* with air temperature but air temperatures tended to be higher for
342 northwesterly as compared to southeasterly cases. At -25°C freezing temperatures for the INPs, most northwesterly samples had
343 a range of INP concentrations at higher air temperatures (i.e., $> -9^{\circ}\text{C}$), while southeasterly samples exhibited overall higher INP
344 concentrations, but still at a range of air temperatures (Figure 6e). In contrast, there was no correlation or gradient relationship
345 between INP concentrations at any temperature and wind speed (Figure 6f–h), unlike the correlation between wind speed and
346 INPs at -8°C observed by Stopelli et al. (2016). We also evaluated INP concentrations versus wind speed at -8°C but did not see
347 any correlation (not shown). Regarding the snow, it is possible that surface processes generate airborne ice particles, which
348 contribute to a snow sample collected at a mountain station (Beck et al., 2018). However, snow that is re-suspended during a
349 snowfall event largely consists of the most recently fallen snow crystals covering wind-exposed surfaces. These particles are
350 unlikely to be different from concurrently falling snow. Hence, their contribution will not change INP abundance or spectral
351 properties of the collected sample. Another matter are hoar frost crystals, which can be very abundant in terms of number, but
352 because of their small size (i.e., $< 100\text{ }\mu\text{m}$ (Lloyd et al., 2015)) can only make a minor contribution to the mass of solid precipitation
353 depositing in a tin placed horizontally on a mountain crest. The majority of small crystals will follow the streamlines of air passing
354 over the crest. All that an increased influence of hoar frost particles would do to our observations is to decrease measured
355 differences between snow and rime samples, because additions of hoar frost, a form of rime, would render the collected snow
356 sample a bit more similar to rime.

357 Figure 7 shows the cumulative and normalized differential INP spectra from the northwesterly and southeasterly case day samples.
358 In addition to containing higher concentrations of warm temperature INPs, more southeasterly samples contained a bimodal
359 distribution relative to the colder and unimodal distributions from northwesterly samples. The warm mode, or “bump” at
360 temperatures above approximately -20°C has been observed in a wide range of previous immersion mode ice nucleation studies
361 including but not limited to some of the earliest studies of total aerosol (Vali, 1971), residuals found in hail (Vali and Stansbury,
362 1966), sea spray aerosol (McCluskey et al., 2017; DeMott et al., 2016), soil samples (Hill et al., 2016), agricultural harvesting
363 emissions (Suski et al., 2018), and in recent reviews of aerosol (Kanji et al., 2017; DeMott et al., 2018) and precipitation (Petters
364 and Wright, 2015) samples. Most previous studies that show spectra with the warm mode typically: (1) report a wide range of
365 freezing temperatures such that it can be observed relative to the steady increase of INPs at colder temperatures (i.e., Figure 7, left
366 column) or (2) are of samples that include a mixture of biological and mineral or other less efficient INP sources. For example,
367 several previous studies report INP concentrations down to only -15°C (e.g., Conen and Yakutin, 2018; Hara et al., 2016; Kieft,
368 1988; Schnell and Vali, 1976; Vali et al., 1976; Wex et al., 2015), namely because the goal was to target efficient, warm-
369 temperature biological INPs. However, the warm mode may not be evident in such studies, given it cannot be visualised next to
370 the drastic increase in INPs with temperatures below -15°C (i.e., the cold mode). In contrast, studies conducting INP measurements
371 on known mineral dust samples also are not able to observe the warm mode (e.g., Price et al., 2018; Atkinson et al., 2013; Murray

et al., 2012). Together, it is apparent that a mixed biological and mineral (or less efficient biological INPs) sample is needed to assess the bimodal behaviour in the INP spectra.

3.3 Potential components of INP populations at JFJ

Taking the spectral characteristics in the context of air mass direction and transport can help elucidate the possible sources of INPs at JFJ during INCAS. Qualitative and quantitative evaluation of the warm mode, or likely, the relative contribution of warm temperature biological INPs, to cold mode INPs is transparent when df/dT and $k(T)$ differential INP spectra are calculated (Figure 6e – g7). Additionally, normalizing such spectra affords a qualitative comparison of spectra signatures between aerosols and residuals found in cloud rime and snow.

~~Figure 8 shows normalized differential spectral characteristics of daily aerosol, rime, and snow INPs.~~ We offer some possible explanations for the observed variability between the samples. Naturally, the boundary layer more frequently than not contains higher concentrations of warm temperature INPs—and INPs in general—as compared to the free troposphere given the proximity to the sources (e.g., forests, agriculture, vegetation, and the oceans) (Burrows et al., 2013; Despres et al., 2012; Frohlich-Nowoisky et al., 2016; Wilson et al., 2015; Burrows et al., 2009a; Burrows et al., 2009b; Frohlich-Nowoisky et al., 2012; Suski et al., 2018). Although, microorganisms and nanoscale biological fragments are episodically lofted into the free troposphere with mineral dust and transported thousands of kilometres (Creamean et al., 2013; Kellogg and Griffin, 2006).

Air arriving at JFJ on 15 and 16 Feb originated from the farthest away and were not heavily exposed to boundary layer air, as evidenced by the air mass trajectory analysis (Figure 3) and radon (Figure 1c5), indicating long-range transport in the free troposphere. This could explain why the warm mode (and higher T_{10} and T_{50}) was observed for in the rime and snow, but not the aerosol—the aerosol had sufficient time to nucleate ice during free tropospheric transport and especially the warm temperature INPs that would likely become depleted in-cloud first (Stopelli et al., 2015), assuming the clouds formed along the air mass transport pathways, as also supported by the higher INP concentrations in most of the rime and snow compared to the aerosol in Figure 6b. Cloud fraction was relatively low (12.5 to 25%), but air temperatures were relatively high (–8.4 to –7.1 °C), suggesting conditions were amenable for long-range transported warm temperature INPs to nucleate cloud ice. However, from the available data, we cannot determine with certainty if the local conditions were the same as those when nucleation initially occurred. For 19 and 20 Feb, air temperature was ~~very~~ cold (–16.4 and –19.6 °C, respectively) cloud fraction was high (92 and 54%, respectively), and all samples ~~remained unimodal did not contain a warm mode (i.e., only containing the cold mode).~~ One possible explanation is that any warm temperature INPs that were present in the clouds had already snowed out prior to reaching the sampling location, as observed by Stopelli et al. (2015) at JFJ. Although, given the low radon concentrations and erratic transport pathways, it is possible such air masses did not contain a relatively large concentrations of warm temperature INPs due to deficient exchange with the boundary layer. It was not until the southeasterly cases that the aerosol samples exhibited ~~bimodal-a warm mode~~ characteristics (i.e., contained both the warm and cold modes). Specifically, on 23 Feb local winds shifted to southeasterly (147 degrees on average) and air masses arrived from over the eastern Alps, Eastern Europe, Scandinavia, and earlier on in time, the Atlantic Ocean. Thus, these samples were predominantly influenced by the continental (mostly over remote regions) and marine boundary layers ~~(Figures 4 and 5),~~ where sources of warm temperature INPs are more abundant (Frohlich-Nowoisky et al., 2016).

The northwesterly case of ~~006~~ Mar is somewhat interesting in that the local wind direction was clearly from the northwest, but air mass source analyses show brief transport in the boundary layer (radon) from the south, when looking farther back in time, traveling over the Mediterranean and North Africa. The aerosol sample had ~~the third-highest~~ a high onset temperature for INPs relative to

other northwest samples (Figure 6b) and snow samples exhibited ~~bimodality~~ a warm mode (Figure 6g-8e). It is the only one of the northwesterly case samples that encountered boundary layer exposure according to the radon observations. Combined, these results suggest a somewhat mixed-source sample, and that 06 Mar may not be directly parallel to the other northwesterly cases. Transitioning back to a southeasterly case on 11 Mar, only the rime and snow unveiled ~~bimodal behaviour~~ a warm mode from air transported from similar regions as the 06 Mar sample. ~~However, transport on 11 Mar was more directly from the south over the Mediterranean and North Africa, indicating less time for removal of the INPs during transport.~~ Additionally, OPSC concentrations were very low (Figure 51c). These results suggest the aerosols already nucleated cloud ice prior to reaching JFJ on 11 Mar (i.e., low ambient aerosol), which is supported by the 10 Mar sampling where the aerosol was bimodal but did not contain a warm mode, but rime and snow did. rime was unimodal, and snow was bimodal, but the warm mode resided at a relatively cold temperature (-16.5°C).

~~Two other days without snowfall support the conclusion that southeasterly air mass transport introduces warm temperature INPs to JFJ. When evaluating the SDE and BLI days, there is a bit of variability.~~ On 24 Feb, clouds were present at JFJ (a cloud fraction of 37.5%), but riming was insufficient to collect a sufficient enough quantity for INP analysis and no snowfall occurred. Interestingly, the warm mode was the maximum second highest for the aerosol sample ~~ce—normally, the cold mode has the highest normalized value—and it did not contain a cold mode (for df/dT).~~ indicating a larger relatively large contribution of warm temperature INPs as compared to the total INP population. Air mass transport was very similar to 23 Feb signifying similar INP sources even though this day was characterized as an SDE, but it is probable that a slightly warmer (-6.0 as compared to -9.8°C air temperature), drier (79 versus 89% relative humidity), and higher pressure (649 versus 645 mb) postfrontal system moved over JFJ on 24 Feb, inhibiting removal of warm temperature INPs during transport relative to the day prior (corroborated by reanalysis from NCEP/NCAR of geopotential height at 600 mb). The ~~second BLI case of~~ 28 Feb (not shown) was very similar to 24 Feb in that: (1) only an aerosol sample was collected and (2) the warm mode was the maximum mode for df/dT . As compared to 27 Feb where a warm mode was not observed, 28 Feb was warmer (-20.0 as compared to -26.2°C), drier (52 versus 62%), higher pressure (635 versus 630 mb), and had a warmer onset temperature (-6.8 versus -14.8°C). Wind direction was slightly different: southeasterly (153 degrees) on 27 Feb as compared to southwesterly on 28 Feb (221 degrees). However, conditions were cloudier than the 23 – 24 Feb coupling and completely cloudy on 27 Feb (100 and 66.7% cloud fraction on 27 Feb and 28 Feb, respectively). Additionally, radon and OPSC concentrations were the highest on 27 – 28 Feb as compared to the rest of the days during INCAS (Figure 1c5). Combined, these results suggest a very local, boundary layer source of INPs started on 27 Feb, but were quickly depleted in the very cloudy conditions. Once clouds started to clear and a shift in frontal characteristics occurred, a similar source of very efficient warm temperature INPs affected JFJ but were able to be observed in the aerosol.

4 Conclusions and broader implications

Aerosol, cloud rime, and snow samples were collected at the High-Altitude Research Station Jungfraujoch during the INCAS field campaign in Feb and Mar 2018. The objectives of the study were to assess variability in wintertime INP sources found in cloudy environments and evaluate relationships between INPs found in the different sample materials. To directly compare air to liquid samples, characteristics of normalized differential fraction frozen and INP spectra were compared in the context of cumulative INP spectra statistics, air mass transport and exposure to boundary layer or free tropospheric conditions, and local meteorology. Distinction between northwesterly and southeasterly conditions yielded variable results regarding INP efficiency and concentrations, biological versus non-biological sources, and meteorological conditions at the sampling location. In general, cumulative INP concentrations were 3 to 20 times higher for all sample types when sources from the southeast infiltrated JFJ,

while the ~~modality of the~~ INP spectra ~~of the aerosol was bimodal~~ contained a warm mode for aerosol but the presence of a warm mode was variable for the rime and snow depending on meteorological context.

In general, comprehensive measurements of INPs from aerosol, and rime and snow when possible, affords useful information to compare and explain exchange between aerosols, clouds, and precipitation in the context of local and regional scale meteorology and transport conditions. Assessment of different INP spectral types, modality, and spectra statistics adds another dimension for qualitative and semi-quantitative intercomparison of sampling days and evaluation of associations between aerosol, cloud, and precipitation sampling. -Extending INP analyses past reporting cumulative concentrations affords more detailed information on the population of INPs and enables comparison between samples from aerosols, clouds, precipitation, and beyond (e.g., seawater, soil, etc.). Using auxiliary measurements and air mass simulations, in addition to context provided by previous work at JFJ, we have addressed possible sources for INCAS. However, more detailed source apportionment work should be imminent to comprehensively characterize INP sources based on spectral features. Future studies should ideally use such statistical analyses in tandem with focused chemical and biological characterization assessments to provide direct linkages between INP spectral properties and sources. Such investigations could yield valuable information on INP sources, and aerosol-cloud-precipitation interactions, which could then be used to improve process-level model parameterizations of such interactions by rendering quantitative information on INP source, efficiency, and abundance. Improving understanding of aerosol impacts on clouds and precipitation will ultimately significantly enhance understanding of the earth system with respect to cloud effects on the surface energy and water budgets to address future concerns of climate change and water availability.

Author contributions

JMC collected the samples, conducted the DFA sample analysis, conducted data analysis, and wrote the manuscript. CM and FC also contributed to collecting rime and snow samples. JMC, CM, and FC designed the experiments. NB provided quality controlled OPS data. CM, NB, and FC helped with manuscript feedback and revision prior to submission.

Acknowledgements

The Swiss National Science Foundation (SNF) financially supported JMC within its Scientific Exchanges Programme, through grant number IZSEZ0_179151. The work of CM and FC on Jungfrauoch is made possible through SNF grant number 200021_169620. Radon measurements were performed as part of the Swiss contribution to ICOS (www.icos-ri.eu). Aerosol data were acquired by Paul Scherrer Institute in the framework of the Global Atmosphere Watch (GAW) programme funded by MeteoSwiss. We would like to thank Gabor Vali, one other anonymous reviewer, and Martin Gysel for their valuable feedback during the review process. Further support was received from the ACTRIS2 project funded through the EU H2020-INFRAIA-2014-2015 programme (grant agreement no. 654109) and the Swiss State Secretariat for Education, Research and Innovation (SERI; contract number 15.0159-1). The opinions expressed and arguments employed herein do not necessarily reflect the official views of the Swiss Government. We are grateful to the International Foundation High Altitude Research Stations Jungfrauoch and Gornergrat (HFSJG), 3012 Bern, Switzerland, for providing through its infrastructure comfortable access to mixed-phase clouds. Special thanks for go to Joan and Martin Fischer, and Christine and Ruedi Käser, the custodians of the station. The authors gratefully acknowledge the NOAA Air Resources Laboratory (ARL) for the provision of the HYSPLIT transport and dispersion model and/or READY website (<http://www.ready.noaa.gov>) used in this publication.

- Albrecht, B. A.: Aerosols, Cloud Microphysics, and Fractional Cloudiness, *Science*, 245, 1227-1230, 10.1126/science.245.4923.1227, 1989.
- Alpert, P. A., Aller, J. Y., and Knopf, D. A.: Ice nucleation from aqueous NaCl droplets with and without marine diatoms, *Atmos. Chem. Phys.*, 11, 5539-5555, 10.5194/acp-11-5539-2011, 2011.
- Atkinson, J. D., Murray, B. J., Woodhouse, M. T., Whale, T. F., Baustian, K. J., Carslaw, K. S., Dobbie, S., O'Sullivan, D., and Malkin, T. L.: The importance of feldspar for ice nucleation by mineral dust in mixed-phase clouds, *Nature*, 498, 355-358, 10.1038/nature12278, 2013.
- Augustin, S., Wex, H., Niedermeier, D., Pummer, B., Grothe, H., Hartmann, S., Tomsche, L., Clauss, T., Voigtländer, J., Ignatius, K., and Stratmann, F.: Immersion freezing of birch pollen washing water, *Atmos. Chem. Phys.*, 13, 10989-11003, 10.5194/acp-13-10989-2013, 2013.
- Baltensperger, U., Gäggeler, H. W., Jost, D. T., Lugauer, M., Schwikowski, M., Weingartner, E., and Seibert, P.: Aerosol climatology at the high-alpine site Jungfraujoch, Switzerland, *Journal of Geophysical Research: Atmospheres*, 102, 19707-19715, doi:10.1029/97JD00928, 1997.
- Beck, A., Henneberger, J., Fugal, J. P., David, R. O., Lacher, L., and Lohmann, U.: Impact of surface and near-surface processes on ice crystal concentrations measured at mountain-top research stations, *Atmos Chem Phys*, 18, 8909-8927, 10.5194/acp-18-8909-2018, 2018.
- Bergeron, T.: On the physics of cloud and precipitation, 5th Assembly of the U.G.G.I., Paul Dupont, Paris, 1935.
- Bigg, E. K.: The Supercooling of Water, *P Phys Soc Lond B*, 66, 688-694, Doi 10.1088/0370-1301/66/8/309, 1953.
- Boose, Y., Sierau, B., Garcia, M. I., Rodriguez, S., Alastuey, A., Linke, C., Schnaiter, M., Kupiszewski, P., Kanji, Z. A., and Lohmann, U.: Ice nucleating particles in the Saharan Air Layer, *Atmos. Chem. Phys.*, 16, 9067-9087, 2016.
- Boucher, O., Randall, D., Artaxo, P., Bretherton, C., Feingold, G., Forster, P., Kerminen, V.-M., Kondo, Y., Liao, H., Lohmann, U., Rasch, P., Satheesh, S. K., Sherwood, S., Stevens, B., and Zhang, X. Y.: Clouds and Aerosols, in: *Climate Change 2013: The Physical Science Basis. Contribution of Working Group I to the Fifth Assessment Report of the Intergovernmental Panel on Climate Change*, edited by: Stocker, T. F., Qin, D., Plattner, G.-K., Tignor, M., Allen, S. K., Boschung, J., Nauels, A., Xia, Y., Bex, V., and Midgley, P. M., Cambridge University Press, Cambridge, United Kingdom and New York, NY, USA, 571-658, 2013.
- Bowers, R. M., Lauber, C. L., Wiedinmyer, C., Hamady, M., Hallar, A. G., Fall, R., Knight, R., and Fierer, N.: Characterization of Airborne Microbial Communities at a High-Elevation Site and Their Potential To Act as Atmospheric Ice Nuclei, *Applied and Environmental Microbiology*, 75, 5121-5130, 10.1128/Aem.00447-09, 2009.
- Bukowiecki, N., Richard, A., Furger, M., Weingartner, E., Aguirre, M., Huthwelker, T., Lienemann, P., Gehrig, R., and Baltensperger, U.: Deposition Uniformity and Particle Size Distribution of Ambient Aerosol Collected with a Rotating Drum Impactor, *Aerosol Science and Technology*, 43, 891-901, 10.1080/02786820903002431, 2009.
- Bukowiecki, N., Weingartner, E., Gysel, M., Coen, M. C., Zieger, P., Herrmann, E., Steinbacher, M., Gäggeler, H. W., and Baltensperger, U.: A Review of More than 20 Years of Aerosol Observation at the High Altitude Research Station Jungfraujoch, Switzerland (3580 m asl), *Aerosol and Air Quality Research*, 16, 764-788, 10.4209/aaqr.2015.05.0305, 2016.
- Burrows, S. M., Butler, T., Jockel, P., Tost, H., Kerkweg, A., Poschl, U., and Lawrence, M. G.: Bacteria in the global atmosphere - Part 2: Modeling of emissions and transport between different ecosystems, *Atmos Chem Phys*, 9, 9281-9297, DOI 10.5194/acp-9-9281-2009, 2009a.
- Burrows, S. M., Elbert, W., Lawrence, M. G., and Poschl, U.: Bacteria in the global atmosphere - Part 1: Review and synthesis of literature data for different ecosystems, *Atmos Chem Phys*, 9, 9263-9280, DOI 10.5194/acp-9-9263-2009, 2009b.
- Burrows, S. M., Hoose, C., Poschl, U., and Lawrence, M. G.: Ice nuclei in marine air: biogenic particles or dust?, *Atmos Chem Phys*, 13, 245-267, 10.5194/acp-13-245-2013, 2013.
- Cahill, T. A., Feeney, P. J., and Eldred, R. A.: Size Time Composition Profile of Aerosols Using the Drum Sampler, *Nucl Instrum Meth B*, 22, 344-348, Doi 10.1016/0168-583x(87)90355-7, 1987.
- Chambers, S. D., Williams, A. G., Conen, F., Griffiths, A. D., Reimann, S., Steinbacher, M., Krummel, P. B., Steele, L. P., van der Schoot, M. V., Galbally, I. E., Molloy, S. B., and Barnes, J. E.: Towards a Universal "Baseline" Characterisation of Air Masses for High- and Low-Altitude Observing Stations Using Radon-222, *Aerosol and Air Quality Research*, 16, 885-899, 10.4209/aaqr.2015.06.0391, 2016.
- Christner, B. C., Morris, C. E., Foreman, C. M., Cai, R. M., and Sands, D. C.: Ubiquity of biological ice nucleators in snowfall, *Science*, 319, 1214-1214, 10.1126/science.1149757, 2008.
- Collaud Coen, M., Weingartner, E., Schaub, D., Hueglin, C., Corrigan, C., Henning, S., Schwikowski, M., and Baltensperger, U.: Saharan dust events at the Jungfraujoch: detection by wavelength dependence of the single scattering albedo and first climatology analysis, *Atmos. Chem. Phys.*, 4, 2465-2480, 2004.
- Collaud Coen, M., Weingartner, E., Furger, M., Nyeki, S., Prevot, A. S. H., Steinbacher, M., and Baltensperger, U.: Aerosol climatology and planetary boundary influence at the Jungfraujoch analyzed by synoptic weather types, *Atmos Chem Phys*, 11, 5931-5944, 10.5194/acp-11-5931-2011, 2011.

540 Collaud Coen, M., Andrews, E., Aliaga, D., Andrade, M., Angelov, H., Bukowiecki, N., Ealo, M., Fialho, P., Flentje, H., Hallar,
541 A. G., Hooda, R., Kalapov, I., Krejci, R., Lin, N.-H., Marinoni, A., Ming, J., Nguyen, N. A., Pandolfi, M., Pont, V., Ries,
542 L., Rodriguez, S., Schauer, G., Sellegri, K., Sharma, S., Sun, J., Tunved, P., Velasquez, P., and Ruffieux, D.: Identification
543 of topographic features influencing aerosol observations at high altitude stations, *Atmos. Chem. Phys.*, 18, 12289-12313,
544 2018.

545 Coluzza, I., Creamean, J., Rossi, M., Wex, H., Alpert, P., Bianco, V., Boose, Y., Dellago, C., Felgitsch, L., Fröhlich-Nowoisky,
546 J., Herrmann, H., Jungblut, S., Kanji, Z., Menzl, G., Moffett, B., Moritz, C., Mutzel, A., Pöschl, U., Schauperl, M., Scheel,
547 J., Stopelli, E., Stratmann, F., Grothe, H., and Schmale, D.: Perspectives on the Future of Ice Nucleation Research:
548 Research Needs and Unanswered Questions Identified from Two International Workshops, *Atmosphere*, 8, 138, 2017.

549 Conen, F., Morris, C. E., Leifeld, J., Yakutin, M. V., and Alewell, C.: Biological residues define the ice nucleation properties of
550 soil dust, *Atmos. Chem. Phys.*, 11, 9643-9648, 10.5194/acp-11-9643-2011, 2011.

551 Conen, F., Rodriguez, S., Hüglin, C., Henne, S., Herrmann, E., Bukowiecki, N., and Alewell, C.: Atmospheric ice nuclei at the
552 high-altitude observatory Jungfraujoch, Switzerland, *Tellus B*, 67, 10.3402/tellusb.v67.25014, 2015.

553 Conen, F., and Yakutin, M. V.: Soils rich in biological ice-nucleating particles abound in ice-nucleating macromolecules likely
554 produced by fungi, *Biogeosciences*, 15, 4381-4385, 10.5194/bg-15-4381-2018, 2018.

555 Creamean, J. M., Suski, K. J., Rosenfeld, D., Cazorla, A., DeMott, P. J., Sullivan, R. C., White, A. B., Ralph, F. M., Minnis, P.,
556 Comstock, J. M., Tomlinson, J. M., and Prather, K. A.: Dust and Biological Aerosols from the Sahara and Asia Influence
557 Precipitation in the Western U.S., *Science*, 339, 1572-1578, DOI 10.1126/science.1227279, 2013.

558 Creamean, J. M., Kirpes, R. M., Pratt, K. A., Spada, N. S., Maahn, M., de Boer, G., Schnell, R. C., and China, S.: Marine and
559 terrestrial influences on ice nucleating particles during continuous springtime measurements in an Arctic oilfield location,
560 *Atmos Chem Phys*, 18, 1-20, <https://doi.org/10.5194/acp-18-1-2018>, 2018a.

561 Creamean, J. M., Primm, K. M., Tolbert, M. A., Hall, E. G., Wendell, J., Jordan, A., Sheridan, P. J., Smith, J., and Schnell, R. C.:
562 HOVERCAT: A novel aerial system for evaluation of aerosol-cloud interactions, *Atmos. Meas. Tech.*, submitted, 2018b.

563 Cziczo, D. J., Ladino, L., Boose, Y., Kanji, Z. A., Kupiszewski, P., Lance, S., Mertes, S., and Wex, H.: Measurements of Ice
564 Nucleating Particles and Ice Residuals, *Meteorological Monographs*, 58, 8.1-8.13, 10.1175/amsmonographs-d-16-0008.1,
565 2017.

566 DeMott, P. J., Chen, Y., Kreidenweis, S. M., Rogers, D. C., and Sherman, D. E.: Ice formation by black carbon particles, *Geophys*
567 *Res Lett*, 26, 2429-2432, Doi 10.1029/1999gl900580, 1999.

568 DeMott, P. J., Prenni, A. J., Liu, X., Kreidenweis, S. M., Petters, M. D., Twohy, C. H., Richardson, M. S., Eidhammer, T., and
569 Rogers, D. C.: Predicting global atmospheric ice nuclei distributions and their impacts on climate, *P Natl Acad Sci USA*,
570 107, 11217-11222, 10.1073/pnas.0910818107, 2010.

571 DeMott, P. J., Hill, T. C. J., McCluskey, C. S., Prather, K. A., Collins, D. B., Sullivan, R. C., Ruppel, M. J., Mason, R. H., Irish,
572 V. E., Lee, T., Hwang, C. Y., Rhee, T. S., Snider, J. R., McMeeking, G. R., Dhaniyala, S., Lewis, E. R., Wentzell, J. J.
573 B., Abbatt, J., Lee, C., Sultana, C. M., Ault, A. P., Axson, J. L., Martinez, M. D., Venero, I., Santos-Figueroa, G., Stokes,
574 M. D., Deane, G. B., Mayol-Bracero, O. L., Grassian, V. H., Bertram, T. H., Bertram, A. K., Moffett, B. F., and Franc,
575 G. D.: Sea spray aerosol as a unique source of ice nucleating particles, *P Natl Acad Sci USA*, 113, 5797-5803,
576 10.1073/pnas.1514034112, 2016.

577 DeMott, P. J., Möhler, O., Cziczo, D. J., Hiranuma, N., Petters, M. D., Petters, S. S., Belosi, F., Bingemer, H. G., Brooks, S. D.,
578 Budke, C., Burkert-Kohn, M., Collier, K. N., Danielczok, A., Eppers, O., Felgitsch, L., Garimella, S., Grothe, H., Herenz,
579 P., Hill, T. C. J., Höhler, K., Kanji, Z. A., Kiselev, A., Koop, T., Kristensen, T. B., Krüger, K., Kulkarni, G., Levin, E. J.
580 T., Murray, B. J., Nicosia, A., D., O. S., A., P., J., P. M., C., P. H., Reicher, N., Rothenberg, D. A., Rudich, Y., Santachiara,
581 G., Schiebel, T., Schrod, J., Seifried, T. M., Stratmann, F., Sullivan, R. C., Suski, K. J., Szakáll, M., Taylor, H. P., Ullrich,
582 R., Vergara-Temprado, J., Wagner, R., Whale, T. F., Weber, D., Welti, A., Wilson, T. W., Wolf, M. J., and Zenker, J.:
583 The Fifth International Workshop on Ice Nucleation phase 2 (FIN-02): Laboratory intercomparison of ice nucleation
584 measurements, *Atmos. Meas. Tech.*, in review, <https://doi.org/10.5194/amt-2018-191>, 2018.

585 Despres, V. R., Huffman, J. A., Burrows, S. M., Hoose, C., Safatov, A. S., Buryak, G., Frohlich-Nowoisky, J., Elbert, W., Andreae,
586 M. O., Poschl, U., and Jaenicke, R.: Primary biological aerosol particles in the atmosphere: a review, *Tellus B*, 64,
587 10.3402/tellusb.v64i0.15598, 2012.

588 Draxler, R. R.: HYSPLIT4 user's guide, NOAA Air Resources Laboratory, Silver Spring, MD., 1999.

589 Draxler, R. R., and Rolph, G.: HYSPLIT (HYbrid Single-Particle Lagrangian Integrated Trajectory) Model access via NOAA ARL
590 READY website (<http://ready.arl.noaa.gov/hysplit.php>), NOAA Air Resources Laboratory, Silver Spring, MD, 2011.

591 Eriksen Hammer, S., Mertes, S., Schneider, J., Ebert, M., Kandler, K., and Weinbruch, S.: Composition of ice particle residuals in
592 mixed-phase clouds at Jungfraujoch (Switzerland): enrichment and depletion of particle groups relative to total aerosol,
593 *Atmos. Chem. Phys.*, 18, 13987-14003, 2018.

594 Fridlind, A. M., Diedenhoven, B. v., Ackerman, A. S., Avramov, A., Mrowiec, A., Morrison, H., Zuidema, P., and Shupe, M. D.:
595 A FIRE-ACE/SHEBA Case Study of Mixed-Phase Arctic Boundary Layer Clouds: Entrainment Rate Limitations on
596 Rapid Primary Ice Nucleation Processes, *Journal of the Atmospheric Sciences*, 69, 365-389, 10.1175/jas-d-11-052.1,
597 2012.

598 Frohlich-Nowoisky, J., Burrows, S. M., Xie, Z., Engling, G., Solomon, P. A., Fraser, M. P., Mayol-Bracero, O. L., Artaxo, P.,
599 Begerow, D., Conrad, R., Andreae, M. O., Despres, V. R., and Poschl, U.: Biogeography in the air: fungal diversity over
600 land and oceans, *Biogeosciences*, 9, 1125-1136, 10.5194/bg-9-1125-2012, 2012.

601 Frohlich-Nowoisky, J., Kampf, C. J., Weber, B., Huffman, J. A., Pohlker, C., Andreae, M. O., Lang-Yona, N., Burrows, S. M.,
602 Gunthe, S. S., Elbert, W., Su, H., Hoor, P., Thines, E., Hoffmann, T., Despres, V. R., and Poschl, U.: Bioaerosols in the
603 Earth system: Climate, health, and ecosystem interactions, *Atmos Res*, 182, 346-376, 10.1016/j.atmosres.2016.07.018,
604 2016.

605 Fröhlich-Nowoisky, J., Hill, T. C. J., Pummer, B. G., Yordanova, P., Franc, G. D., and Pöschl, U.: Ice nucleation activity in the
606 widespread soil fungus *Mortierella alpina*, *Biogeosciences*, 12, 1057-1071, 10.5194/bg-12-1057-2015, 2015.

607 Ganguly, M., Dib, S., and Ariya, P. A.: Purely Inorganic Highly Efficient Ice Nucleating Particle, *ACS Omega*, 3, 3384-3395,
608 10.1021/acsomega.7b01830, 2018.

609 Griffiths, A. D., Conen, F., Weingartner, E., Zimmermann, L., Chambers, S. D., Williams, A. G., and Steinbacher, M.: Surface-
610 to-mountaintop transport characterised by radon observations at the Jungfraujoch, *Atmos Chem Phys*, 14, 12763-12779,
611 10.5194/acp-14-12763-2014, 2014.

612 Hader, J. D., Wright, T. P., and Petters, M. D.: Contribution of pollen to atmospheric ice nuclei concentrations, *Atmos. Chem.*
613 *Phys.*, 14, 5433-5449, 10.5194/acp-14-5433-2014, 2014a.

614 Hader, J. D., Wright, T. P., and Petters, M. D.: Contribution of pollen to atmospheric ice nuclei concentrations, *Atmos Chem Phys*,
615 14, 5433-5449, 10.5194/acp-14-5433-2014, 2014b.

616 Hara, K., Maki, T., Kakikawa, M., Kobayashi, F., and Matsuki, A.: Effects of different temperature treatments on biological ice
617 nuclei in snow samples, *Atmos Environ*, 140, 415-419, 10.1016/j.atmosenv.2016.06.011, 2016.

618 Herrmann, E., Weingartner, E., Henne, S., Vuilleumier, L., Bukowiecki, N., Steinbacher, M., Conen, F., Coen, M. C., Hammer,
619 E., Juranyi, Z., Baltensperger, U., and Gysel, M.: Analysis of long-term aerosol size distribution data from Jungfraujoch
620 with emphasis on free tropospheric conditions, cloud influence, and air mass transport, *J Geophys Res-Atmos*, 120, 9459-
621 9480, 10.1002/2015jd023660, 2015.

622 Hill, T. C. J., DeMott, P. J., Tobo, Y., Fröhlich-Nowoisky, J., Moffett, B. F., Franc, G. D., and Kreidenweis, S. M.: Sources of
623 organic ice nucleating particles in soils, *Atmos. Chem. Phys.*, 16, 7195-7211, 10.5194/acp-16-7195-2016, 2016.

624 Hoose, C., and Möhler, O.: Heterogeneous ice nucleation on atmospheric aerosols: a review of results from laboratory experiments,
625 *Atmos. Chem. Phys.*, 12, 9817-9854, 10.5194/acp-12-9817-2012, 2012.

626 Hu, W., Niu, H. Y., Murata, K., Wu, Z. J., Hu, M., Kojima, T., and Zhang, D. Z.: Bacteria in atmospheric waters: Detection,
627 characteristics and implications, *Atmos Environ*, 179, 201-221, 10.1016/j.atmosenv.2018.02.026, 2018.

628 Hummel, M., Hoose, C., Gallagher, M., Healy, D. A., Huffman, J. A., O'Connor, D., Poschl, U., Pohlker, C., Robinson, N. H.,
629 Schnaiter, M., Sodeau, J. R., Stengel, M., Toprak, E., and Vogel, H.: Regional-scale simulations of fungal spore aerosols
630 using an emission parameterization adapted to local measurements of fluorescent biological aerosol particles, *Atmos*
631 *Chem Phys*, 15, 6127-6146, 10.5194/acp-15-6127-2015, 2015.

632 Jaenicke, R.: Atmospheric aerosols and global climate, *Journal of Aerosol Science*, 11, 577-588, [https://doi.org/10.1016/0021-](https://doi.org/10.1016/0021-8502(80)90131-7)
633 [8502\(80\)90131-7](https://doi.org/10.1016/0021-8502(80)90131-7), 1980.

634 Jaenicke, R.: Abundance of Cellular Material and Proteins in the Atmosphere, *Science*, 308, 73-73, 10.1126/science.1106335,
635 2005.

636 Jaenicke, R., Matthias-Maser, S., and Gruber, S.: Omnipresence of biological material in the atmosphere, *Environmental*
637 *Chemistry*, 4, 217-220, <https://doi.org/10.1071/EN07021>, 2007.

638 Kanji, Z. A., Ladino, L. A., Wex, H., Boose, Y., Burkert-Kohn, M., Cziczo, D. J., and Krämer, M.: Overview of Ice Nucleating
639 Particles, *Meteorological Monographs*, 58, 1.1-1.33, 10.1175/amsmonographs-d-16-0006.1, 2017.

640 Kellogg, C. A., and Griffin, D. W.: Aerobiology and the global transport of desert dust, *Trends Ecol Evol*, 21, 638-644,
641 10.1016/j.tree.2006.07.004, 2006.

642 Kieft, T. L.: Ice Nucleation Activity in Lichens, *Applied and Environmental Microbiology*, 54, 1678-1681, 1988.

643 Knopf, D. A., Alpert, P. A., Wang, B., and Aller, J. Y.: Stimulation of ice nucleation by marine diatoms, *Nature Geoscience*, 4,
644 88, 10.1038/ngeo1037, 2010.

645 Korolev, A., McFarquhar, G., Field, P. R., Franklin, C., Lawson, P., Wang, Z., Williams, E., Abel, S. J., Axisa, D., Borrmann, S.,
646 Crosier, J., Fugal, J., Krämer, M., Lohmann, U., Schlenczek, O., Schnaiter, M., and Wendisch, M.: Mixed-Phase Clouds:
647 Progress and Challenges, *Meteorological Monographs*, 58, 5.1-5.50, 10.1175/amsmonographs-d-17-0001.1, 2017.

648 Lacher, L., Lohmann, U., Boose, Y., Zipori, A., Herrmann, E., Bukowiecki, N., Steinbacher, M., and Kanji, Z. A.: The Horizontal
649 Ice Nucleation Chamber (HINC): INP measurements at conditions relevant for mixed-phase clouds at the High Altitude
650 Research Station Jungfraujoch, *Atmos. Chem. Phys.*, 17, 15199-15224, <https://doi.org/10.5194/acp-17-15199-2017>,
651 2017.

652 Lacher, L., DeMott, P. J., Levin, E. J. T., Suski, K. J., Boose, Y., Zipori, A., Herrmann, E., Bukowiecki, N., Steinbacher, M., Gute,
653 E., Abbatt, J. P. D., Lohmann, U., and Kanji, Z. A.: Background Free-Tropospheric Ice Nucleating Particle Concentrations
654 at Mixed-Phase Cloud Conditions, *Journal of Geophysical Research: Atmospheres*, 123, doi:10.1029/2018JD028338,
655 2018a.

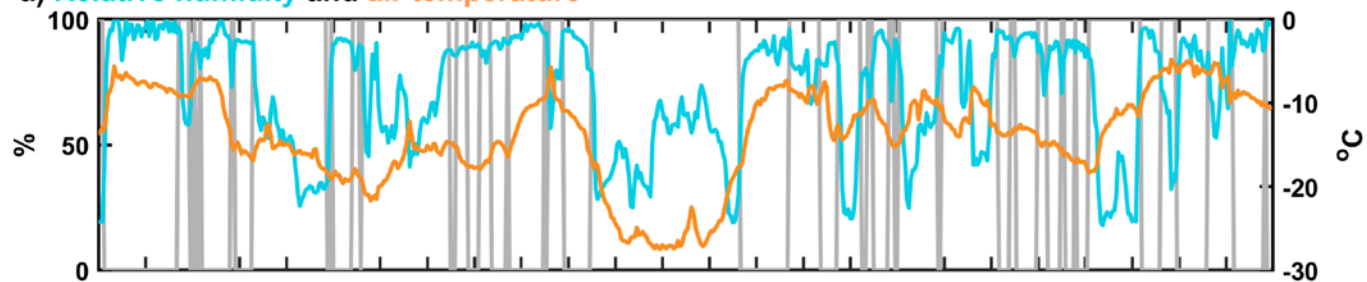
656 Lacher, L., Steinbacher, M., Bukowiecki, N., Herrmann, E., Zipori, A., and Kanji, Z. A.: Impact of Air Mass Conditions and
 657 Aerosol Properties on Ice Nucleating Particle Concentrations at the High Altitude Research Station Jungfraujoch,
 658 Atmosphere, 9, 2018b.
 659 Langham, E. J., and Mason, B. J.: The Heterogeneous and Homogeneous Nucleation of Supercooled Water, *Proc R Soc Lon Ser-*
 660 *A*, 247, 493-&, DOI 10.1098/rspa.1958.0207, 1958.
 661 Lloyd, G., Choularton, T. W., Bower, K. N., Gallagher, M. W., Connolly, P. J., Flynn, M., Farrington, R., Crosier, J., Schlenczek,
 662 O., Fugal, J., and Henneberger, J.: The origins of ice crystals measured in mixed-phase clouds at the high-alpine site
 663 Jungfraujoch, *Atmos Chem Phys*, 15, 12953-12969, 10.5194/acp-15-12953-2015, 2015.
 664 Lohmann, U., Henneberger, J., Henneberg, O., Fugal, J. P., Bühl, J., and Kanji, Z. A.: Persistence of orographic mixed-phase
 665 clouds, *Geophys Res Lett*, 43, 10,512-510,519, doi:10.1002/2016GL071036, 2016.
 666 Mason, R. H., Si, M., Chou, C., Irish, V. E., Dickie, R., Elizondo, P., Wong, R., Brintnell, M., Elsassner, M., Lassar, W. M., Pierce,
 667 K. M., Leaitch, W. R., MacDonald, A. M., Platt, A., Toom-Sauntry, D., Sarda-Esteve, R., Schiller, C. L., Suski, K. J.,
 668 Hill, T. C. J., Abbatt, J. P. D., Huffman, J. A., DeMott, P. J., and Bertram, A. K.: Size-resolved measurements of ice-
 669 nucleating particles at six locations in North America and one in Europe, *Atmos Chem Phys*, 16, 1637-1651, 10.5194/acp-
 670 16-1637-2016, 2016.
 671 McCluskey, C. S., Hill, T. C. J., Malfatti, F., Sultana, C. M., Lee, C., Santander, M. V., Beall, C. M., Moore, K. A., Cornwell, G.
 672 C., Collins, D. B., Prather, K. A., Jayarathne, T., Stone, E. A., Azam, F., Kreidenweis, S. M., and DeMott, P. J.: A
 673 Dynamic Link between Ice Nucleating Particles Released in Nascent Sea Spray Aerosol and Oceanic Biological Activity
 674 during Two Mesocosm Experiments, *Journal of the Atmospheric Sciences*, 74, 151-166, 10.1175/Jas-D-16-0087.1, 2017.
 675 Mignani, C., Creamean, J. M., Zimmermann, L., Alewell, C., and Conen, F.: Direct evidence for secondary ice formation at around
 676 -15 °C in mixed-phase clouds, *Atmos. Chem. Phys. Discuss.*, under review, 2018.
 677 Morris, C. E., Georgakopoulos, D. G., and Sands, D. C.: Ice nucleation active bacteria and their potential role in precipitation, *J*
 678 *Phys Iv*, 121, 87-103, DOI 10.1051/jp4:2004121004, 2004.
 679 Morris, C. E., Sands, D. C., Bardin, M., Jaenicke, R., Vogel, B., Leyronas, C., Ariya, P. A., and Psenner, R.: Microbiology and
 680 atmospheric processes: research challenges concerning the impact of airborne micro-organisms on the atmosphere and
 681 climate, *Biogeosciences*, 8, 17-25, 10.5194/bg-8-17-2011, 2011.
 682 Morris, C. E., Conen, F., Huffman, J. A., Phillips, V., Poschl, U., and Sands, D. C.: Bioprecipitation: a feedback cycle linking
 683 Earth history, ecosystem dynamics and land use through biological ice nucleators in the atmosphere, *Global Change Biol*,
 684 20, 341-351, 10.1111/gcb.12447, 2014.
 685 Morris, C. E., Soubeyrand, S., Bigg, E. K., Creamean, J. M., and Sands, D. C.: Mapping Rainfall Feedback to Reveal the Potential
 686 Sensitivity of Precipitation to Biological Aerosols, *Bulletin of the American Meteorological Society*, 98, 1109-1118,
 687 <https://doi.org/10.1175/BAMS-D-15-00293.1>, 2017.
 688 Mossop, S. C., and Thorndike, N. S. C.: The Use of Membrane Filters in Measurements of Ice Nucleus Concentration. I. Effect of
 689 Sampled Air Volume, *Journal of Applied Meteorology*, 5, 474-480, 10.1175/1520-
 690 0450(1966)005<0474:tuomfi>2.0.co;2, 1966.
 691 Murray, B. J., O'Sullivan, D., Atkinson, J. D., and Webb, M. E.: Ice nucleation by particles immersed in supercooled cloud droplets,
 692 *Chem Soc Rev*, 41, 6519-6554, Doi 10.1039/C2cs35200a, 2012.
 693 O'Sullivan, D., Murray, B. J., Malkin, T. L., Whale, T. F., Umo, N. S., Atkinson, J. D., Price, H. C., Baustian, K. J., Browse, J.,
 694 and Webb, M. E.: Ice nucleation by fertile soil dusts: relative importance of mineral and biogenic components, *Atmos.*
 695 *Chem. Phys.*, 14, 1853-1867, 10.5194/acp-14-1853-2014, 2014.
 696 O'Sullivan, D., Murray, B. J., Ross, J. F., and Webb, M. E.: The adsorption of fungal ice-nucleating proteins on mineral dusts: a
 697 terrestrial reservoir of atmospheric ice-nucleating particles, *Atmos Chem Phys*, 16, 7879-7887, 10.5194/acp-16-7879-
 698 2016, 2016.
 699 Petters, M. D., and Wright, T. P.: Revisiting ice nucleation from precipitation samples, *Geophys Res Lett*, 42, 8758-8766,
 700 10.1002/2015gl065733, 2015.
 701 Price, H. C., Baustian, K. J., McQuaid, J. B., Blyth, A., Bower, K. N., Choularton, T., Cotton, R. J., Cui, Z., Field, P. R., Gallagher,
 702 M., Hawker, R., Merrington, A., Miltenberger, A., Neely, R. R., Parker, S. T., Rosenberg, P. D., Taylor, J. W., Trembath,
 703 J., Vergara-Temprado, J., Whale, T. F., Wilson, T. W., Young, G., and Murray, B. J.: Atmospheric Ice-Nucleating
 704 Particles in the Dusty Tropical Atlantic, *J Geophys Res-Atmos*, 123, 2175-2193, 10.1002/2017jd027560, 2018.
 705 Reche, I., D'Orta, G., Mladenov, N., Winget, D. M., and Suttle, C. A.: Deposition rates of viruses and bacteria above the
 706 atmospheric boundary layer, *Isme J*, 12, 1154-1162, 10.1038/s41396-017-0042-4, 2018.
 707 Sahyoun, M., Korsholm, U. S., Sorensen, J. H., Santl-Temkiv, T., Finster, K., Gosewinkel, U., and Nielsen, N. W.: Impact of
 708 bacterial ice nucleating particles on weather predicted by a numerical weather prediction model, *Atmos Environ*, 170, 33-
 709 44, 10.1016/j.atmosenv.2017.09.029, 2017.
 710 Schnell, R. C., and Vali, G.: Biogenic Ice Nuclei .1. Terrestrial and Marine Sources, *Journal of the Atmospheric Sciences*, 33,
 711 1554-1564, Doi 10.1175/1520-0469(1976)033<1554:Binpit>2.0.Co;2, 1976.
 712 Stein, A. F., Draxler, R. R., Rolph, G. D., Stunder, B. J. B., Cohen, M. D., and Ngan, F.: NOAA's HYSPLIT Atmospheric Transport
 713 and Dispersion Modeling System, *Bulletin of the American Meteorological Society*, 96, 2059-2077, 10.1175/bams-d-14-
 714 00110.1, 2015.

- Stopelli, E., Conen, F., Zimmermann, L., Alewell, C., and Morris, C. E.: Freezing nucleation apparatus puts new slant on study of biological ice nucleators in precipitation, *Atmos Meas Tech*, 7, 129-134, 10.5194/amt-7-129-2014, 2014.
- Stopelli, E., Conen, F., Morris, C. E., Herrmann, E., Bukowiecki, N., and Alewell, C.: Ice nucleation active particles are efficiently removed by precipitating clouds, *Scientific Reports*, 5, 16433, 10.1038/srep16433, 2015.
- Stopelli, E., Conen, F., Morris, C. E., Herrmann, E., Henne, S., Steinbacher, M., and Alewell, C.: Predicting abundance and variability of ice nucleating particles in precipitation at the high-altitude observatory Jungfraujoch, *Atmos Chem Phys*, 16, 8341-8351, 10.5194/acp-16-8341-2016, 2016.
- Stopelli, E., Conen, F., Guilbaud, C., Zopfi, J., Alewell, C., and Morris, C. E.: Ice nucleators, bacterial cells and *Pseudomonas syringae* in precipitation at Jungfraujoch, *Biogeosciences*, 14, 1189-1196, 10.5194/bg-14-1189-2017, 2017.
- Storelvmo, T., Hoose, C., and Eriksson, P.: Global modeling of mixed-phase clouds: The albedo and lifetime effects of aerosols, *Journal of Geophysical Research: Atmospheres*, 116, doi:10.1029/2010JD014724, 2011.
- Suski, K. J., Hill, T. C. J., Levin, E. J. T., Miller, A., DeMott, P. J., and Kreidenweis, S. M.: Agricultural harvesting emissions of ice-nucleating particles, *Atmos. Chem. Phys.*, 18, 13755-13771, 2018.
- Tesson, S. V. M., Skj  th, C. A.,   antl-Temkiv, T., and L  ndahl, J.: Airborne Microalgae: Insights, Opportunities and Challenges, *Applied and Environmental Microbiology*, 10.1128/aem.03333-15, 2016.
- Tobo, Y., DeMott, P. J., Hill, T. C. J., Prenni, A. J., Swoboda-Colberg, N. G., Franc, G. D., and Kreidenweis, S. M.: Organic matter matters for ice nuclei of agricultural soil origin, *Atmos. Chem. Phys.*, 14, 8521-8531, 10.5194/acp-14-8521-2014, 2014.
- Tobo, Y.: An improved approach for measuring immersion freezing in large droplets over a wide temperature range, *Scientific Reports*, 6, ARTN 3293010.1038/srep32930, 2016.
- Twohy, C. H., McMeeking, G. R., DeMott, P. J., McCluskey, C. S., Hill, T. C. J., Burrows, S. M., Kulkarni, G. R., Tanarhte, M., Kafle, D. N., and Toohey, D. W.: Abundance of fluorescent biological aerosol particles at temperatures conducive to the formation of mixed-phase and cirrus clouds, *Atmos Chem Phys*, 16, 8205-8225, 10.5194/acp-16-8205-2016, 2016.
- Twomey, S.: The Influence of Pollution on the Shortwave Albedo of Clouds, *Journal of the Atmospheric Sciences*, 34, 1149-1152, 10.1175/1520-0469(1977)034<1149:tiopot>2.0.co;2, 1977.
- Vali, G., and Stansbury, E. J.: Time-Dependent Characteristics of Heterogeneous Nucleation of Ice, *Can J Phys*, 44, 477-+, DOI 10.1139/p66-044, 1966.
- Vali, G.: Quantitative Evaluation of Experimental Results an the Heterogeneous Freezing Nucleation of Supercooled Liquids, *Journal of the Atmospheric Sciences*, 28, 402-409, 10.1175/1520-0469(1971)028<0402:qeora>2.0.co;2, 1971.
- Vali, G., Christensen, M., Fresh, R. W., Galyan, E. L., Maki, L. R., and Schnell, R. C.: Biogenic Ice Nuclei .2. Bacterial Sources, *Journal of the Atmospheric Sciences*, 33, 1565-1570, Doi 10.1175/1520-0469(1976)033<1565:Binpib>2.0.Co;2, 1976.
- Vali, G., DeMott, P. J., M  hler, O., and Whale, T. F.: Technical Note: A proposal for ice nucleation terminology, *Atmos. Chem. Phys.*, 15, 10263-10270, 10.5194/acp-15-10263-2015, 2015.
- Vali, G.: Revisiting the differential freezing nucleus spectra derived from drop freezing experiments; methods of calculation, applications and confidence limits, *Atmos. Meas. Tech. Discuss.*, 2018, 1-18, 10.5194/amt-2018-309, 2018.
- von Blohn, N., Mitra, S. K., Diehl, K., and Borrmann, S.: The ice nucleating ability of pollen: Part III: New laboratory studies in immersion and contact freezing modes including more pollen types, *Atmos Res*, 78, 182-189, 10.1016/j.atmosres.2005.03.008, 2005.
- Weingartner, E., Nyeki, S., and Baltensperger, U.: Seasonal and diurnal variation of aerosol size distributions ($10 < D < 750$ nm) at a high-alpine site (Jungfraujoch 3580 m asl), *J Geophys Res-Atmos*, 104, 26809-26820, Doi 10.1029/1999jd900170, 1999.
- Wex, H., Augustin-Bauditz, S., Boose, Y., Budke, C., Curtius, J., Diehl, K., Dreyer, A., Frank, F., Hartmann, S., Hiranuma, N., Jantsch, E., Kanji, Z. A., Kiselev, A., Koop, T., Mohler, O., Niedermeier, D., Nillius, B., Rosch, M., Rose, D., Schmidt, C., Steinke, I., and Stratmann, F.: Intercomparing different devices for the investigation of ice nucleating particles using Snomax (R) as test substance, *Atmos Chem Phys*, 15, 1463-1485, 10.5194/acp-15-1463-2015, 2015.
- Wilson, T. W., Ladino, L. A., Alpert, P. A., Breckels, M. N., Brooks, I. M., Browse, J., Burrows, S. M., Carslaw, K. S., Huffman, J. A., Judd, C., Kilthau, W. P., Mason, R. H., McFiggans, G., Miller, L. A., Najera, J. J., Polishchuk, E., Rae, S., Schiller, C. L., Si, M., Temprado, J. V., Whale, T. F., Wong, J. P. S., Wurl, O., Yakobi-Hancock, J. D., Abbatt, J. P. D., Aller, J. Y., Bertram, A. K., Knopf, D. A., and Murray, B. J.: A marine biogenic source of atmospheric ice-nucleating particles, *Nature*, 525, 234-+, 10.1038/nature14986, 2015.
- Wright, T. P., and Petters, M. D.: The role of time in heterogeneous freezing nucleation, *J Geophys Res-Atmos*, 118, 3731-3743, 10.1002/jgrd.50365, 2013.

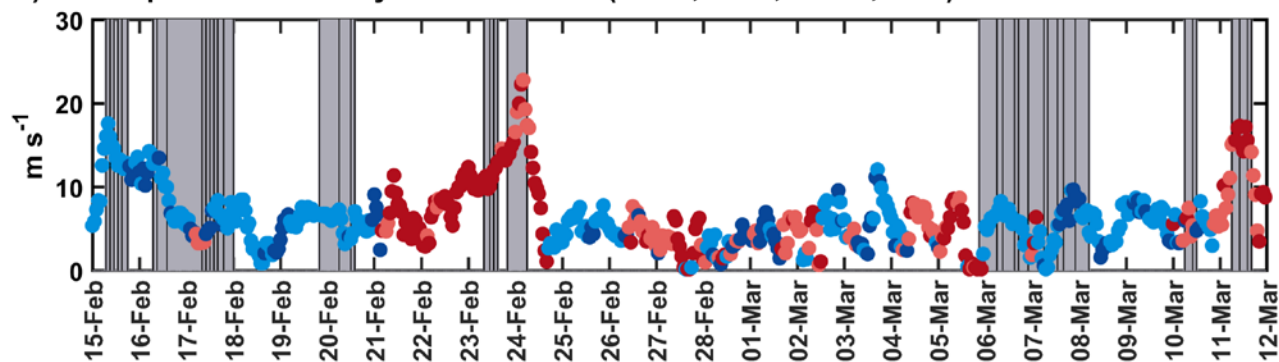
Table 1. Dates and times for cloud rime, snow, and aerosol samples collected during the 2018 winter INCAS study at Jungfraujoch. Also shown are the dominant air mass sources (free troposphere or FT or boundary layer intrusion of BLI) for each day based on radon data. Samples highlighted in blue and red are the northwest and southeast case studies, respectively. Samples highlighted in green represent predominantly southerly days that were classified as Saharan dust events (SDEs) or BLI days.

DateDate	Air mass	Cloud rime		Snow			Aerosol				
		Sample	Start (UTC)	Duration (hh:mm)	Sample	Start (UTC)	Duration (hh:mm)	Sample	Start (UTC)	Duration (hh:mm)	Stages
15-Feb	FT	Rime1	06:30	03:07	Snow1	07:15	01:15	DRUM1	10:00	12:00	A/B/C/D
		Rime2	09:37	02:13	Snow2	08:40	01:30	DRUM2	22:00	24:00	A/B/C/D
		Rime3	11:50	03:55	Snow3	10:10	01:35				
		Rime4	15:45	03:35	Snow4	12:45	02:30				
		Rime5	19:20	13:55	Snow5	15:20	04:00				
16-Feb	FT	Rime6	07:15	02:10	Snow6	07:15	02:02	DRUM3	22:00	24:00	A/B/C/D
		Rime7	09:29	02:41	Snow7	09:23	02:37				
					Snow8	14:00	17:50				
17-Feb	FT	Rime8	12:08	01:16	Snow9	07:50	02:23	DRUM4	22:00	24:00	A/B/C/D
		Rime9	13:24	02:23	Snow10	10:16	01:10				
		Rime10	15:47	03:12	Snow11	11:35	00:33				
		Rime11	18:59	06:48	Snow12	12:20	01:04				
					Snow13	13:42	01:00				
					Snow14	14:45	00:55				
					Snow15	15:54	02:54				
18-Feb	FT	Rime12	00:47	08:22	None			DRUM5	22:00	24:00	A/B/C
19-Feb	FT	Rime13	21:00	10:50	Snow17	21:00	08:50	DRUM6	22:00	24:00	A/B/C
20-Feb	FT	Rime14	05:50	04:14	Snow18	05:50	04:14	DRUM7	22:00	24:00	A/B/C
		Rime15	12:08	02:17	Snow19	12:08	02:14				
21-Feb	FT	None			None			DRUM8	22:00	24:00	A/B/C/D
22-Feb	BLI	None			None			DRUM9	22:00	24:00	A/B/C/D
23-Feb	BLI	Rime16	20:00	14:30	Snow20	07:49	02:51	DRUM10	22:00	24:00	A/B/C/D
					Snow21	10:55	03:35				
					Snow22	14:40	02:42				
					Snow23	20:00	12:11				
24-Feb	FT, SDE	None			None			DRUM11	22:00	24:00	A/B/C
25-Feb	FT	None			None			DRUM12	22:00	24:00	A/B
26-Feb	FT	None			None			DRUM13	22:00	24:00	A/B/C
27-Feb	BLI	None			None			DRUM14	22:00	24:00	A/B/C
28-Feb	BLI	None			None			DRUM15	22:00	24:00	A/B/C
01-Mar	BLI	None			None			DRUM16	22:00	24:00	A/B/C
02-Mar	FT	None			None			DRUM17	22:00	24:00	A/B/C
03-Mar	FT	None			None			DRUM18	22:00	24:00	A/B/C
04-Mar	FT	None			None			DRUM19	22:00	24:00	A/B/C
05-Mar	FT	Rime17	16:43	15:32	Snow24	21:52	08:16	DRUM20	22:00	24:00	A/B/C
06-Mar	BLI	Rime18	06:15	03:03	Snow25	06:15	02:50	DRUM21	22:00	24:00	A/B/C
		Rime19	09:18	05:42	Snow26	09:14	05:26				
		Rime20	15:00	02:08	Snow27	14:54	01:56				
		Rime21	17:08	04:41	Snow28	17:26	04:04				
		Rime22	22:38	21:40	Snow29	22:38	07:35				
07-Mar	BLI	Rime23	06:19	03:58	Snow30	06:19	01:19	DRUM22	22:00	24:00	A/B/C
		Rime24	10:17	05:40	Snow31	07:50	02:00				
		Rime25	15:57	08:31	Snow32	12:49	02:59				
		Rime26	22:28	06:34	Snow33	16:00	05:19				
08-Mar	FT	None			None			DRUM23	22:00	24:00	A/B/C
09-Mar	FT	None			None			DRUM24	22:00	24:00	A/B/C
10-Mar	FT, SDE	Rime27	11:00	21:46	Snow35	06:00	04:00	DRUM25	22:00	24:00	A/B/C
					Snow36	10:10	01:56				
11-Mar	BLI	Rime28	06:46	02:59	Snow37	05:48	04:03	None			
		Rime29	09:56	03:49	Snow38	09:54	03:51				
		Rime30	13:45	04:48	Snow39	13:48	02:28				

a) Relative humidity and air temperature



b) Wind speed coloured by wind direction (north, west, south, east)



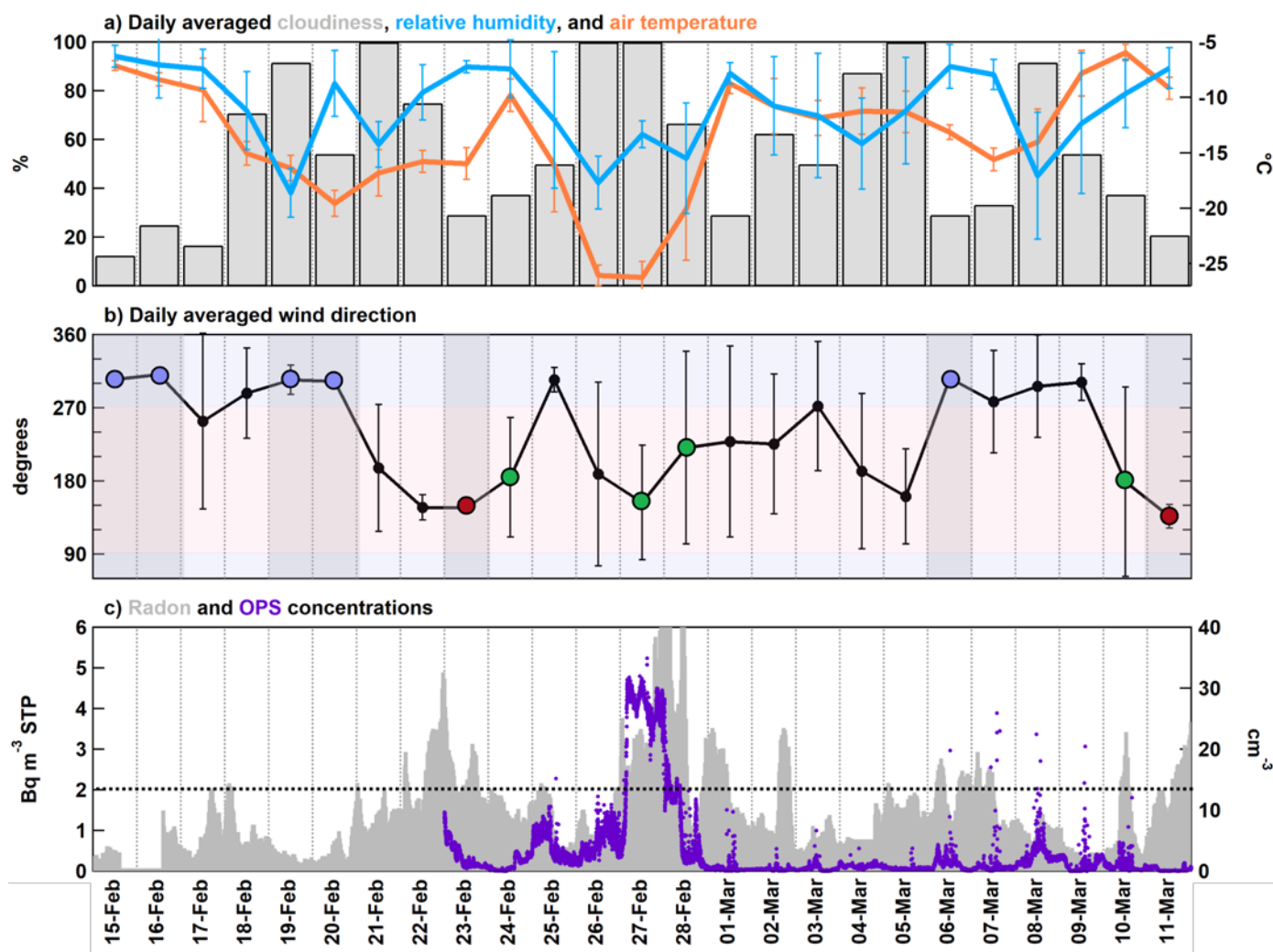


Figure 1. Daily averaged meteorological data at JFJ from INCAS, including a) percentage of cloudiness in the vertical profile over JFJ per the estimation by Herrmann et al. (2015), station relative humidity (%), and station air temperature (°C) and b) station wind direction. The background of b) is shaded horizontally by north (light blue) or south (light red) directions. Additionally, days with combined aerosol, cloud rime, and snow collections are vertically shaded grey. Blue and red markers for wind direction represent case study storm days that were entirely northwesterly or southeasterly, respectively. Green markers represent predominantly southerly days that were classified as Saharan dust events (SDEs) or heavy boundary layer influence days. c) Time series of radon (^{222}Rn) corrected for standard temperature and pressure and OPS particle concentrations. The black dashed line indicates a threshold of 2 Bq m^{-3} whereby boundary layer intrusion likely occurred at JFJ. OPS data were missing prior to 23 Feb. Error bars represent standard deviation. Relative humidity and surface air temperature and b) wind speed colored by wind direction. Grey shading in a) indicates in-cloud measurement conditions per the estimation by Herrmann et al. (2015) and in b) indicates snow and cloud rime collections with the width of the bar indicating the duration of each sample. Aerosol sampling was conducted daily during all conditions (i.e., precipitation, cloudy, and clear sky). North, east, south, and west correspond to wind direction ranges of 315–45, 45–135, 135–225, and 225–315 degrees, respectively.

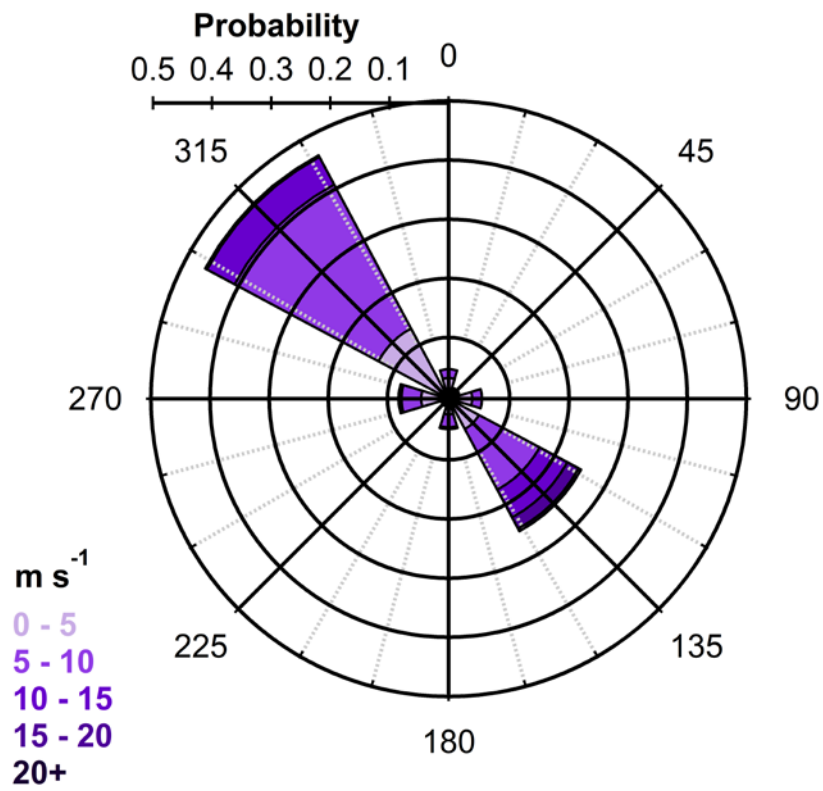
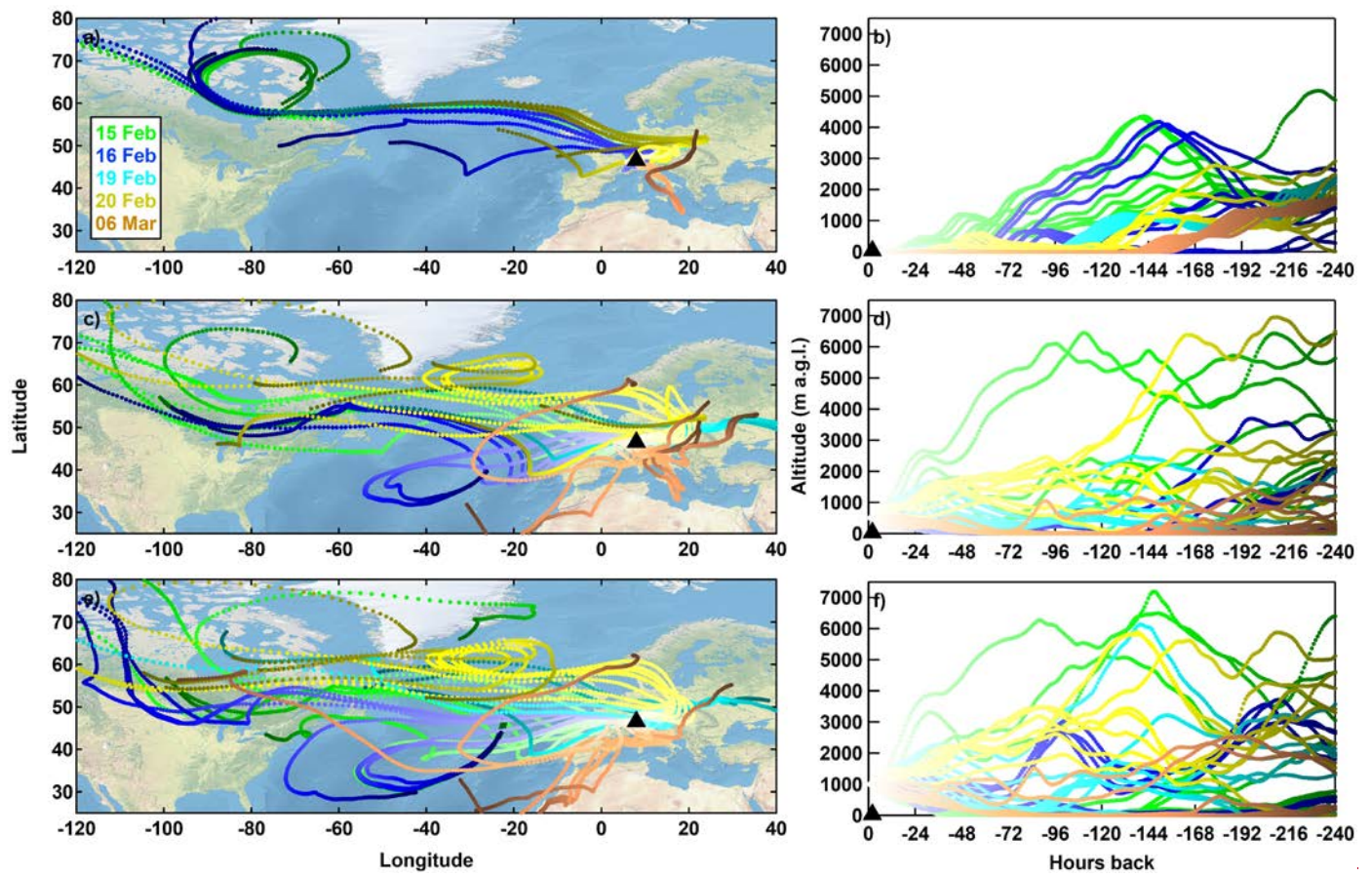


Figure 2. Rose plot for wind data during INCAS. Values correspond to wind direction binned by 45 degrees and wind speeds binned by 5 m s⁻¹. The probability for wind speed to fall within these bins is plotted.



791

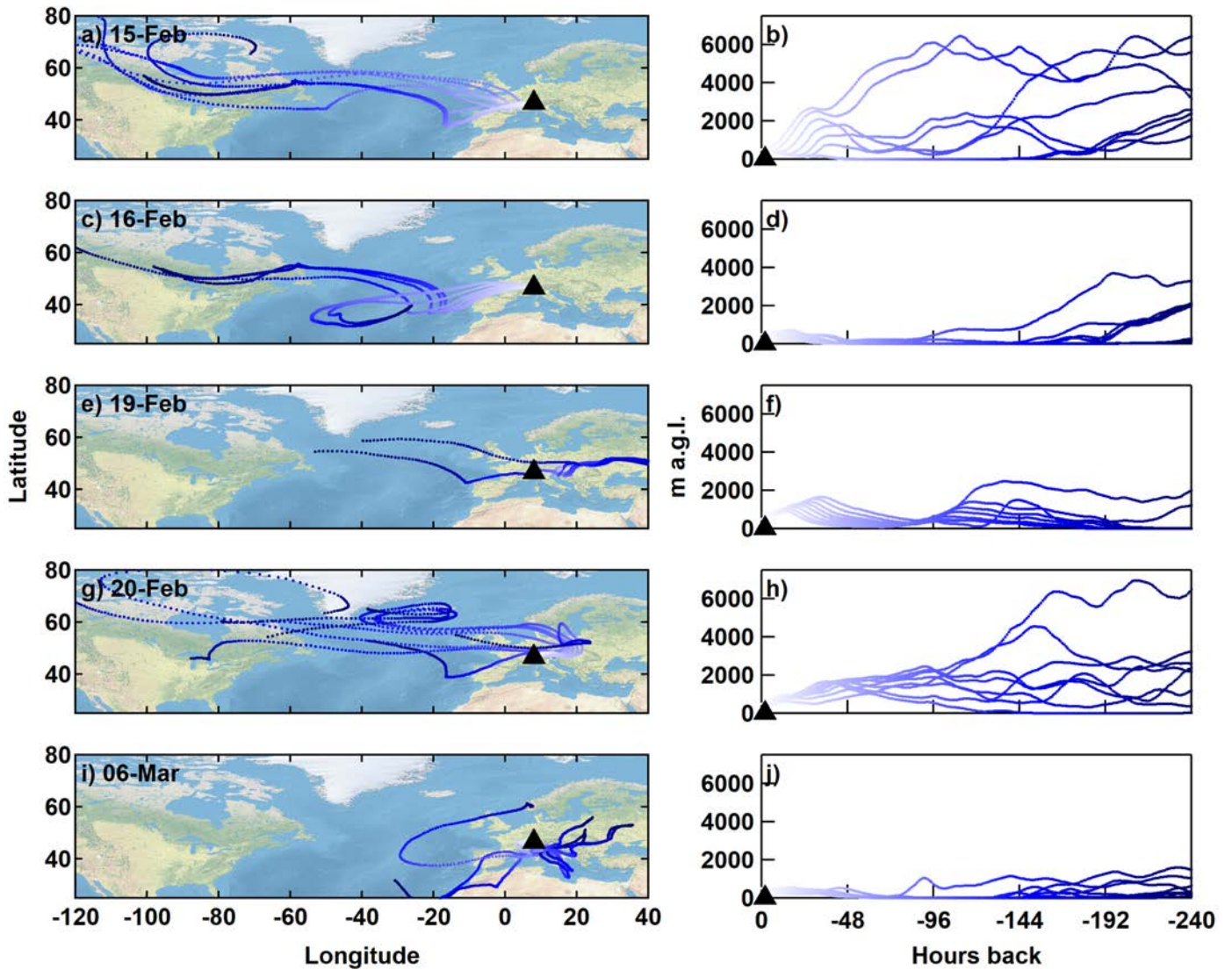
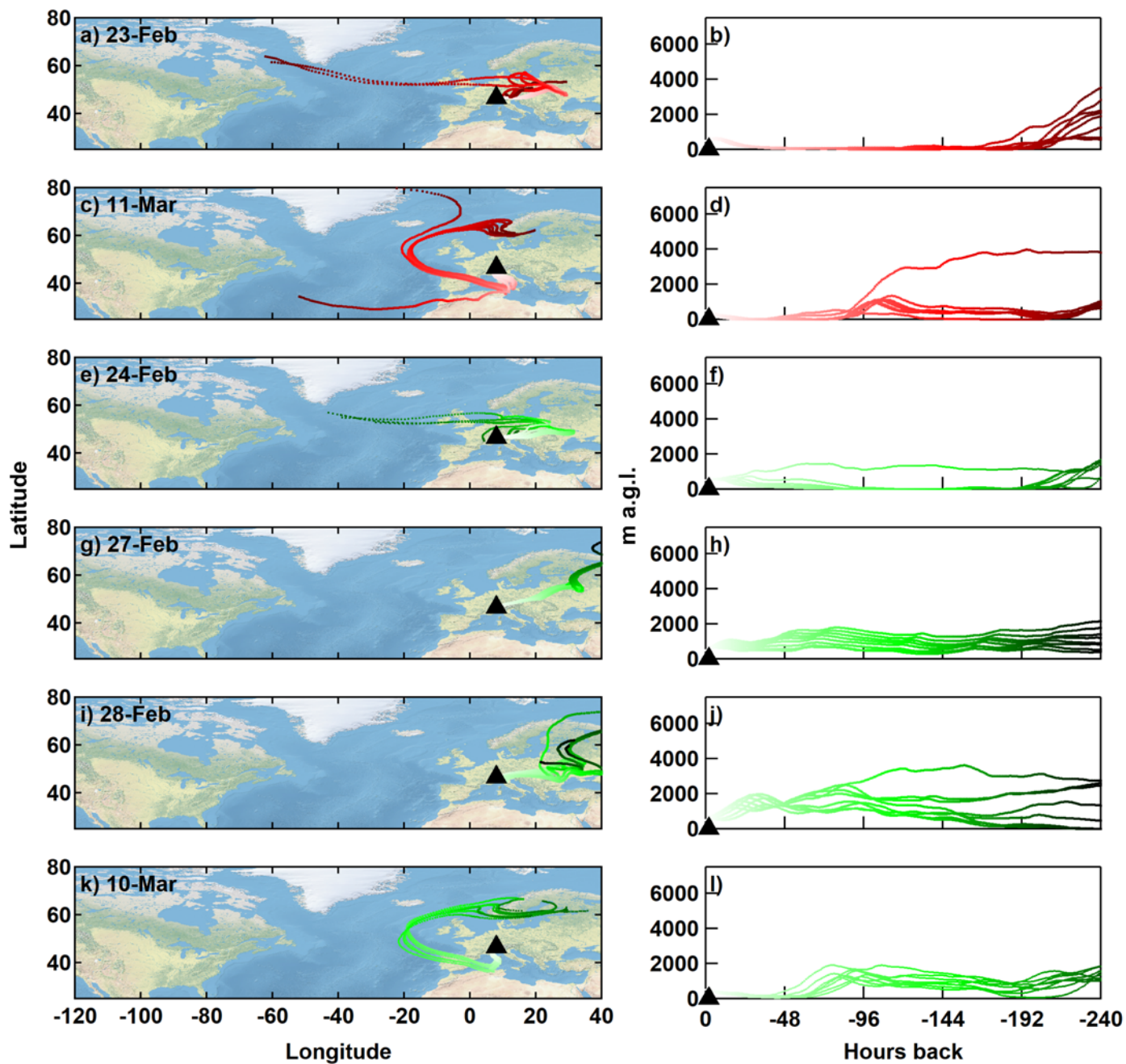


Figure 3. 10-day air mass backward trajectories initiated every 3 hours during sample collection for northwesterly case days ending at 500 m above ground level (a.g.l.). Trajectories are plotted by latitude-longitude (left) and altitude-time (right) profiles for 15 Feb (a, b), 16 Feb (c, d), 19 Feb (e, f), 20 Feb (g, h), and 06 Mar (i, j). Darker shades of blue represent trajectory points farther back in time. at a) 10, e) 500, and i) 1000 m a.g.l. Altitude profiles versus time are also shown for b) 10, d) 500, and f) 1000 m a.g.l. Each day is coloured differently to differentiate between the days.



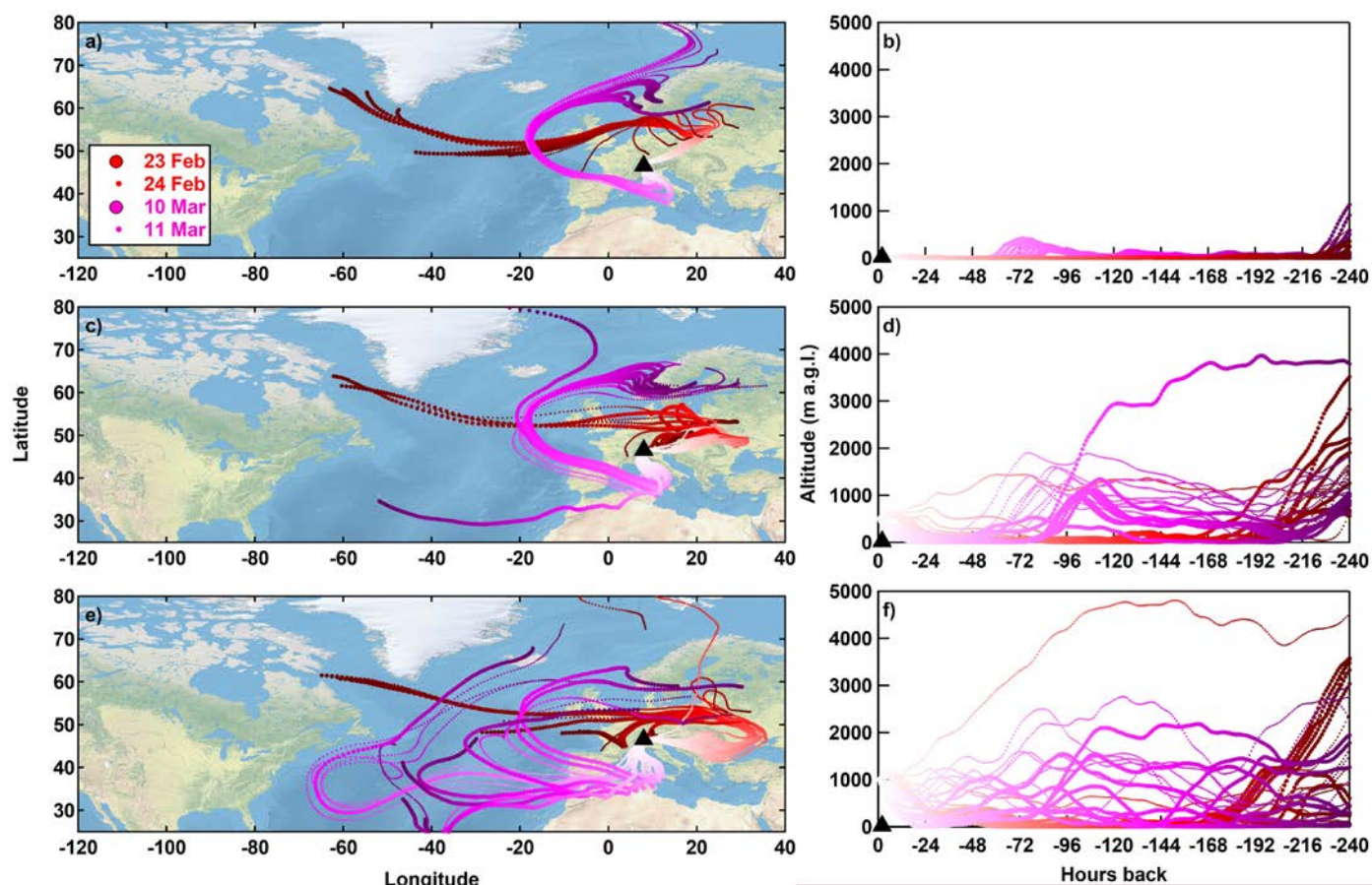


Figure 4. Same as Figure 3, but for southeasterly (23 Feb and 11 Mar), SDE (24 Feb and 10 Mar), and BLI (27 and 28 Feb) -case days. 24 Feb and 10 Mar are shown as smaller markers, indicative of possible Saharan dust events from Paul Scherrer Institute.

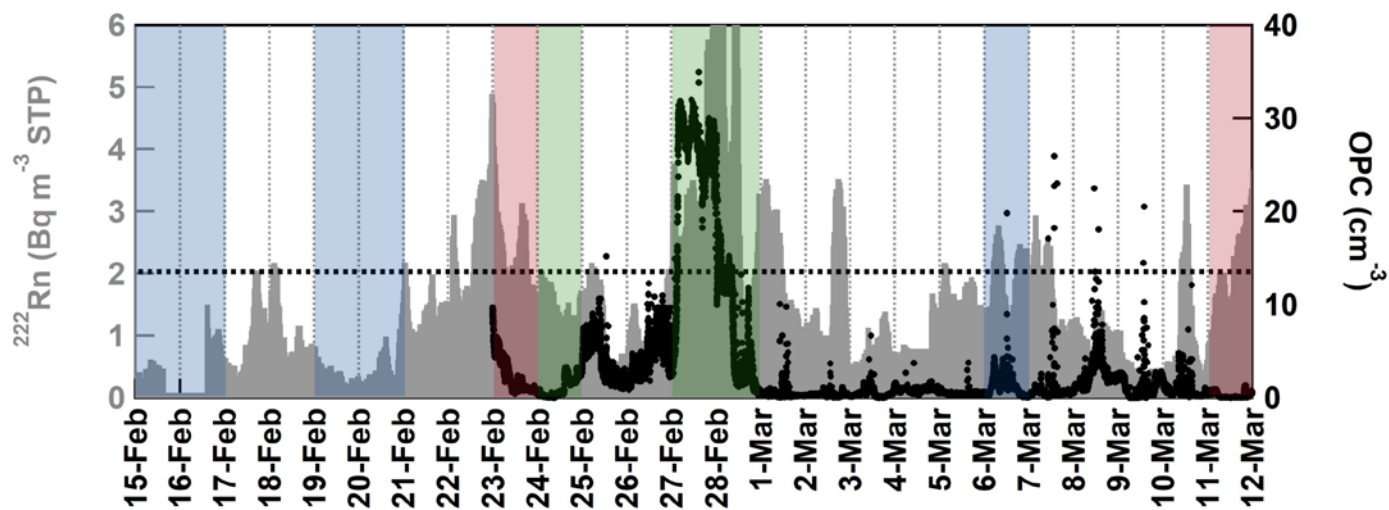


Figure 5. ^{222}Rn concentrations (grey) measured and corrected for standard temperature and pressure during INCAS. OPC particle number concentrations (black) are also shown, but data were missing prior to 23 Feb. The black dashed line indicates a threshold of 2 Bq m^{-3} whereby boundary layer intrusion likely occurred at JFJ. Blue and red shadings represent northwesterly and southeasterly case study days, respectively.

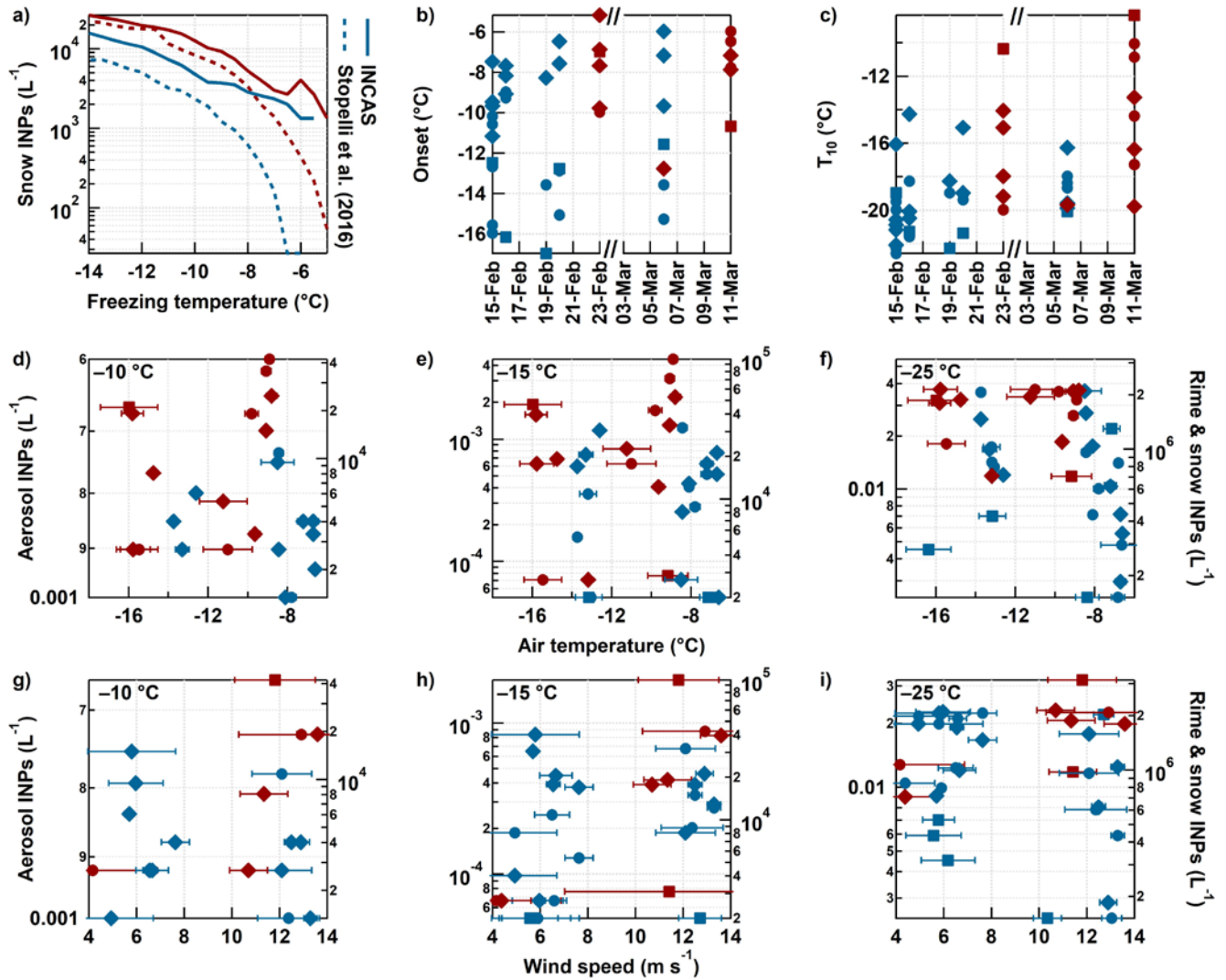
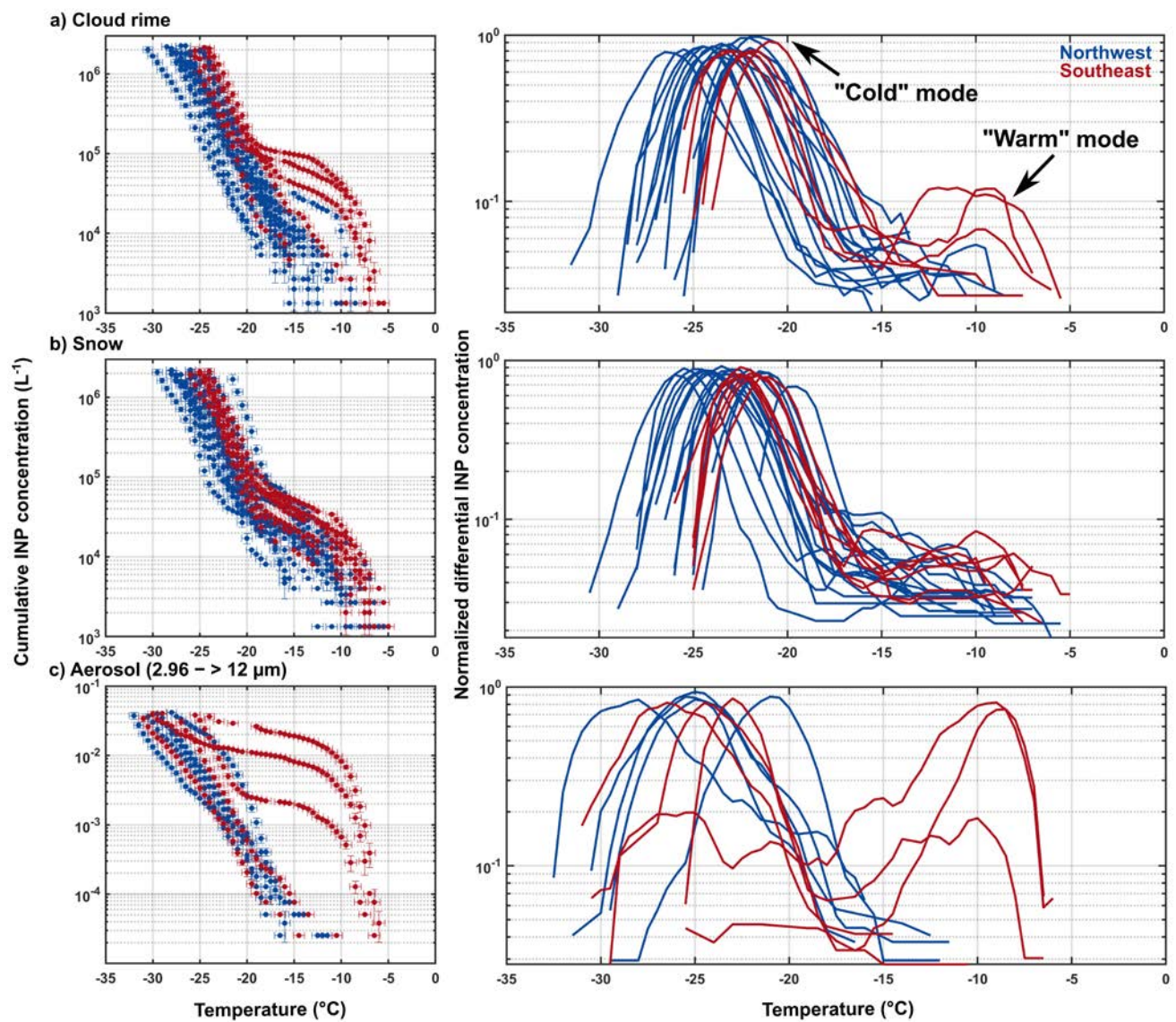


Figure 6. a) Comparison of INCAS snow INPs within the same range of those reported by Stopelli et al. (2016) for measurements at JFJ during the 2012/13 winter season. Summary of INCAS INP concentrations from aerosol (squares), cloud rime (open circles), and snow samples (x's), including b) freezing onset temperatures, and correlations between air temperature averages during sample collection and INPs at freezing temperatures of c) -10°C , d) -15°C , and e) -25°C . The same concentrations at f) -10°C , g) -15°C , and h) -25°C are plotted against average wind speed measured during sample collection periods. Blue and red markers represent northwesterly and southeasterly wind directions, respectively.



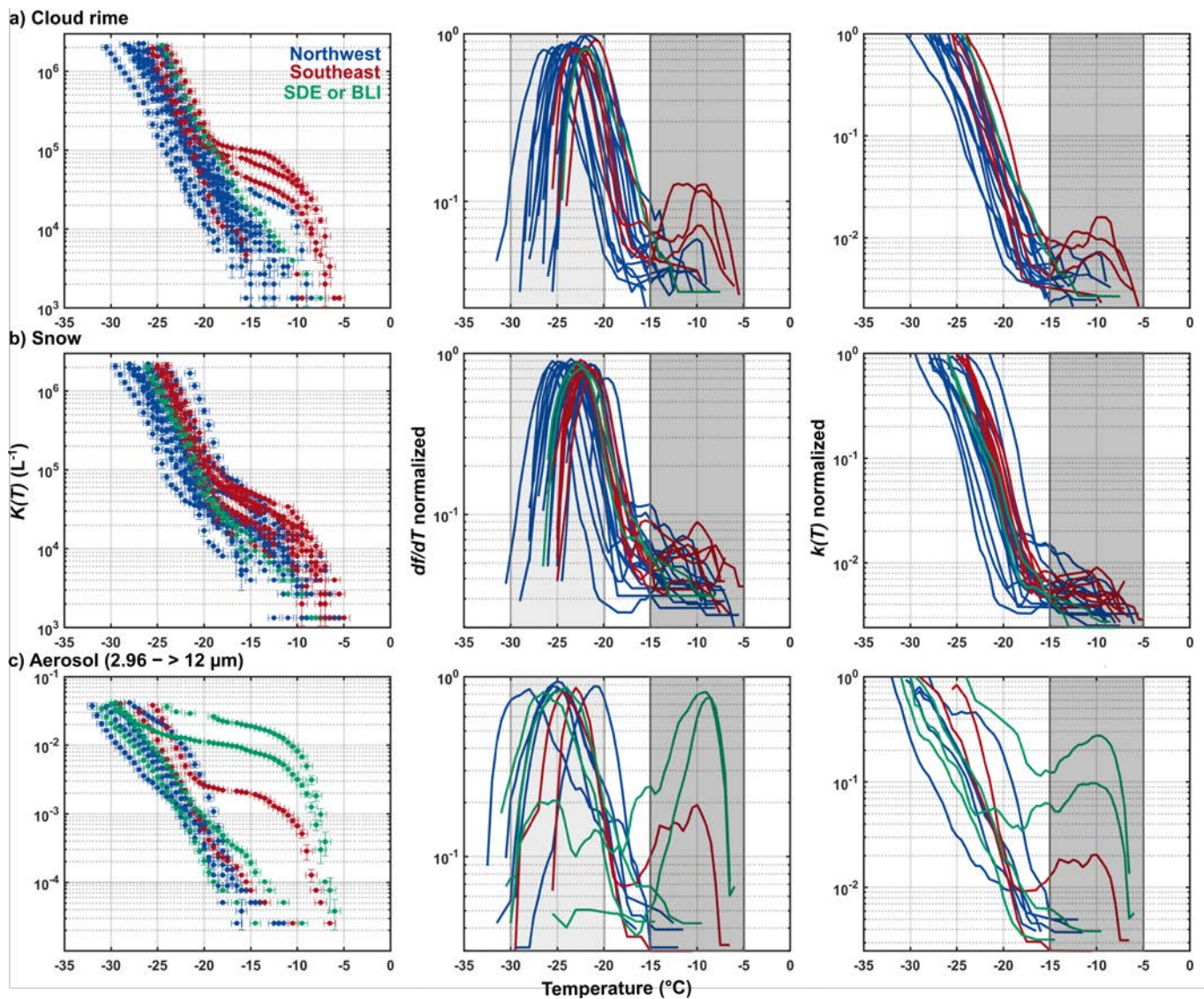


Figure 75. Cumulative INP spectra ($K(T)$), normalized differential of fraction frozen per temperature interval (df/dT), and normalized differential INP spectra ($k(T)$) for the same samples of a) cloud rime, b) snow, and c) aerosol for the size range $2.96 - > 12 \mu\text{m}$ in diameter. Spectra shown are for samples from the northwest (blue) and southeast (red) case study dates, in addition to SDE and boundary layer intrusion (BLI) case days (green). Multiple cloud rime and snow samples were collected while one aerosol sample from each size range was collected on northwest and southeast case study days (see Table 1). Additional dates with only aerosol samples (24 Feb and 27 Feb) are also shown in c) (highest of the two modes $> -15^\circ\text{C}$) and are discussed in section 3.3. The “cold” and “warm” modes are indicated by the dark grey shading in both the normalized df/dT and $k(T)$ INP spectra for cloud rime, for reference, while the cold mode region (for df/dT only) is shown in the normalized df/dT spectra.

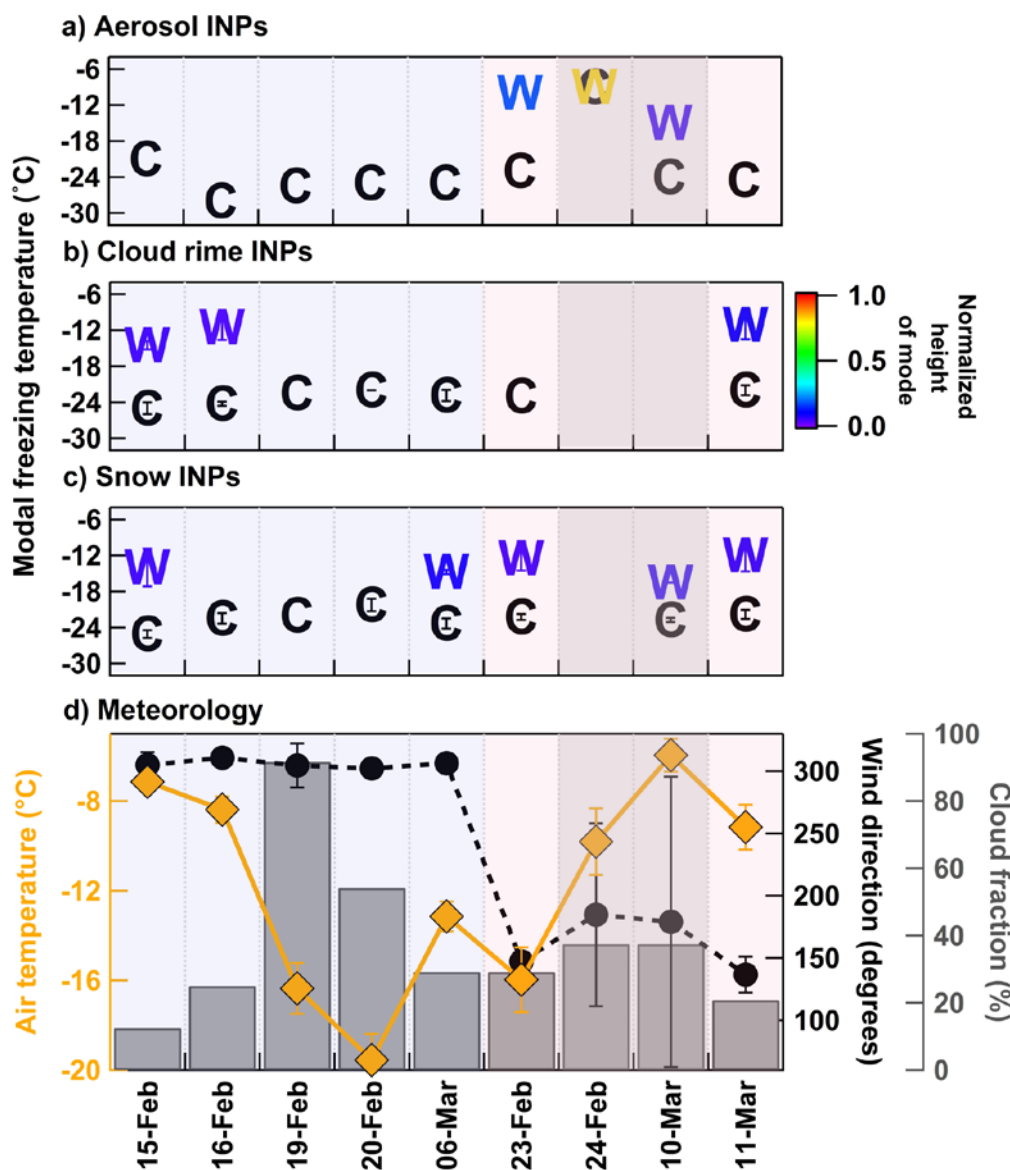
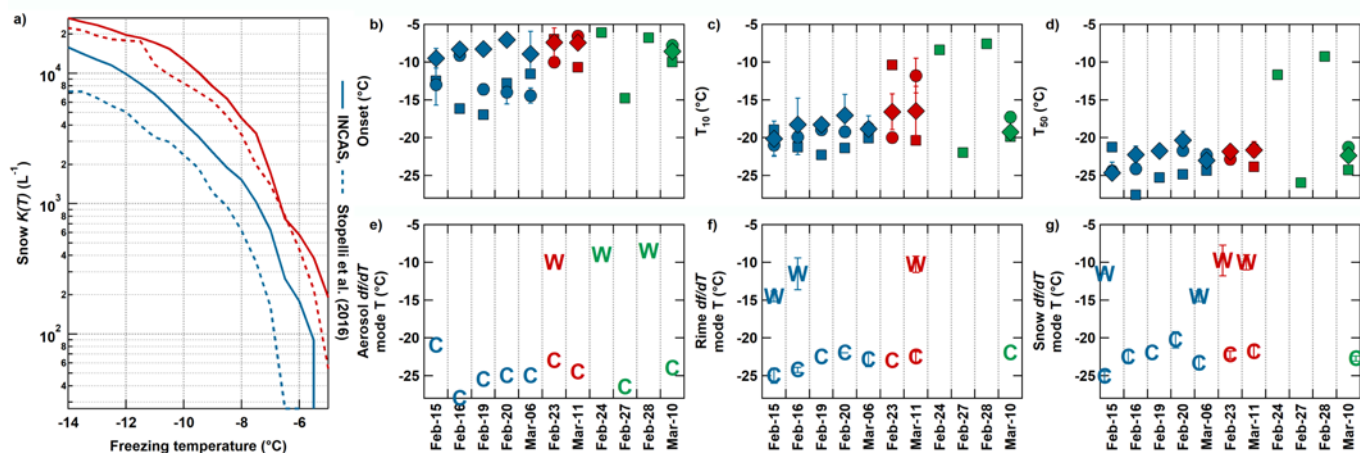


Figure 6. a) Comparison of INCAS cumulative snow INP concentrations for northwest (blue) and southeast (red) within the same range of those reported by Stopelli et al. (2016) for measurements at JFJ during the 2012/13 winter season. Summary of INCAS INP concentrations from aerosol (squares), cloud rime (circles), and snow samples (diamonds), including b) freezing onset temperatures, c) the temperature in which 10% of drops froze, and d) the temperature in which 50% of the drops froze calculated from fraction frozen.

831 From the df/dT spectra, cold and warm mode temperatures are shown for e) aerosol, f) rime, and g) snow samples. The warm mode
832 temperatures from df/dT are the same as for $k(T)$. Blue, red, and green markers represent northwesterly cases, southeasterly cases, and
833 SDE and BLI case days, respectively. Some data points overlap and thus plots may appear to not have the same number of points per
834 sample. Figure 8. Spectral statistics of cold mode height temperature and warm mode height temperatures denoted by “C” and “W”,
835 respectively for a) $2.96 \rightarrow 12 \mu\text{m}$ aerosol, b) cloud rime averaged per day, and c) snow averaged per day. Days with only “C” marker
836 indicate the absence of a warm mode. d) shows average air temperature, wind direction, and cloud fraction during the case study days.
837 The days are ordered by northwesterly (blue shading) and southeasterly (pink shading) case days. The southeasterly cases shaded in
838 grey represent days that were not case study days, but days that help explain circumstances of the sampling on 23 Feb and 11 Mar.